

ABNORMAL VERTICAL PUMP SUCTION RECIRCULATION PROBLEMS DUE TO PUMP-SYSTEM INTERACTION

by

Bruno Schiavello

Director for Fluid Dynamics

Flowserve Pump Division, Technology Department

Phillipsburg, New Jersey

Donald R. Smith

Senior Staff Engineer

and

Stephen M. Price

Senior Staff Engineer

Engineering Dynamics Inc.

San Antonio, Texas



Bruno Schiavello has been Director for Fluid Dynamics at Flowserve Pump Division, Technology Department, in Phillipsburg, New Jersey, since 2000, and previously served in the same position with Ingersoll Dresser Pump Company. He started in the R&D Department of Worthington Nord (Italy), joined Central R&D of Worthington, McGraw Edison Company, and then Dresser Pump Division.

Mr. Schiavello was co-winner of the H. Worthington European Technical Award in 1979. He has written several papers and lectured at seminars in the area of pump recirculation, cavitation, and two-phase flow. He is a member of ASME, AIAA, Societe Hydrotechnique de France, and the International Association for Hydraulic Research. He has served on the International Pump Users Symposium Advisory Committee since 1983.

Mr. Schiavello received a B.S. degree (Mechanical Engineering, 1974) from the University of Rome, and an M.S. degree (Fluid Dynamics, 1975) from Von Karman Institute for Fluid Dynamics, Rhode St. Genese, Belgium.



Donald R. Smith is a Senior Staff Engineer at Engineering Dynamics Incorporated (EDI), in San Antonio, Texas. For the past 30 years, he has been active in the field engineering services, specializing in the analysis of vibration, pulsation, and noise problems with rotating and reciprocating equipment. He has authored and presented several technical papers. Prior to joining EDI, he worked at Southwest Research Institute for 15 years as a Senior

Research Scientist, where he was also involved in troubleshooting and failure analysis of piping and machinery.

Mr. Smith received his B.S. degree (Physics, 1969) from Trinity University. He is a member of ASME and the Vibration Institute.



Stephen M. Price is a Senior Staff Engineer for Engineering Dynamics Inc., in San Antonio, Texas. For the past 19 years, he has been actively involved in solving a variety of problems in systems that have experienced failures due to dynamic phenomenon. He has had field and analytical experience solving problems with reciprocating and rotating machinery, along with structural and acoustical problems. Additionally, Mr. Price has been

involved in development of multiple channel data acquisition and monitoring hardware and software for critical environments. He has presented and published several papers in the areas of signal processing, finite element analysis, fatigue analysis, acoustics, and reciprocating pumps.

Mr. Price has a B.S. degree (Mechanical Engineering) from Mississippi State University and an M.S. degree (Mechanical Engineering) from Purdue University. He is a registered Professional Engineer in the State of Texas and a member of ASME.

ABSTRACT

It is well documented that the proper operation of vertical centrifugal pumps is greatly dependent upon the entire pump/piping system, which includes the piping geometry and the system operating conditions. Oftentimes, pumps operate satisfactorily during shop tests but experience problems after they are installed in the field.

Here, three large vertical pumps that operated satisfactorily on the test stand experienced excessive vibration after installation. Additionally, pulsation in the system piping was found to be causing unexpected vibration in downstream equipment. It was discovered that the problems were the result of complex interaction between several phenomena. Improper inlet conditions caused suction recirculation that generated broadband turbulence. The turbulent energy excited acoustical resonances of the pump/piping system, resulting in pulsation at several discrete frequencies. This energy subsequently excited mechanical natural frequencies of the

motor/pump/piping system causing high amplitude nonsynchronous vibration of the pump and other structures far downstream from the pump.

Field data are presented. Diagnostic techniques and instrumentation needed to obtain the field data required to solve these problems are discussed. Also, additional data from pump hydraulic analysis and sump model tests are presented. Further, the solution strategy with two-step field changes (sump and pump) is shown. Following these modifications, the pumps have operated satisfactorily for more than four years.

INTRODUCTION

The overall pumping system for the condenser circulation cooling water in power stations is formed by three subsystems:

- Suction system,
- Circulation pumps, and
- Discharge system.

A field problem of strong flow induced vibrations and other collateral effects involving the dynamic interaction of all three subsystems is presented in this paper.

Suction System—Intake

The suction system is formed by the intake and the pump pits (sumps). The suction intake typically has a forebay, where the water is conveyed from a large cool water source (sea, lake, or river) into either an open channel with free surface flow, or into a closed conduit.

In the second case, which is the configuration dealt with in this paper, there is a main collector from which the cool water is distributed into each pump pit using individual elbows or T-branches. The main feature of this configuration is that the fluid circulates inside these components as pressurized flow streams with the peculiar characteristics of so called “internal flows.”

In this configuration, the Reynolds number (Re) has the utmost influence. The physical meaning is that $Re = (\text{inertia force}/\text{viscous force})$, which indicates that flows in pipes and elbows with high Re values tend to maintain their streamline pattern (direction, velocity profile, separation zones, and jet characteristics), unless external dissipative forces are applied. In particular, the jet-flow coming out from the exit of the elbow (T-connection) and discharging into the sump has a strong tendency to persist as a jet stream instead of diffusing over the full width of the sump to provide a uniform flow profile as required by the pump (Karassik, et al., 2001). Moreover, the jet is mostly oriented toward one side of the sump due to flow separation inside the elbow causing a solid body rotation in the sump, which may be transferred at the impeller inlet.

Usually, these characteristics are prevented by installing devices inside the sump such as a curtain wall with proper clearance at the bottom, or even a full-height wall with holes (perforated plate) where the primary objectives are to dissipate the energy of the jet-stream and to “regenerate” a uniform velocity profile. This fluid dynamic process of energy dissipation (viscous forces) and velocity pattern reformation (inertia forces) that takes place in the sump space between the discharge mouth of the elbow and the curtain wall/perforated plate is clearly governed by the Reynolds number and Dean number (De), where $De = Re \times (\text{centrifugal force}/\text{inertial force})$. In addition, turning vanes are sometimes used inside the inlet elbow to prevent flow separation and to provide an exit-jet respecting the main symmetry of the sump that is more easily regenerated into a uniform symmetrical profile across the sump width (Blevins, 1984; Idelcik, 1969; Miller, 1979).

Suction System—Sump

A large number of field problems have been experienced in the pump industry with both vertical and horizontal centrifugal pumps where the suction systems include sumps. The study and solutions

of these cases, which included field-lab data and also theoretical investigation, have identified several specific hydraulic phenomena that can have negative impacts on the pumps (performance and reliability) and plant availability (Flowserve-IDP, 1991; Knauss, 1987). These phenomena, which must not be present to an excessive degree (ANSI/HI 9.8, 1998), are:

- Free-surfaces vortices (originating at free water level)
- Submerged vortices (originating at solid boundaries, floor and back/side walls)
- Excessive preswirl of flow entering the pump
- Nonuniform spatial distribution of flow velocity at the impeller eye
- Excessive variation in velocity swirl with time
- Entrained air or gas bubbles

The above phenomena constitute a primary concern for the system designer, pump designer, and pump user. The relative adverse influence on the pump's behavior (vibrations, performance loss, and noise) and plant operation depends primarily upon the physical features of the pump (size, specific speed, hydraulic-mechanical design features), and also upon the plant operating parameters (sump geometry, water level-submergence and net positive suction head available [NPSHA], primary and runout capacity in relation to pump best efficiency point [BEP], and number of pumps in service).

Design Guidelines for Sumps

Presently, guidelines have been established for preventing such phenomena, or minimizing the undesired effects (Prosser, 1977; Flowserve-IDP, 1991; ANSI/HI 9.8, 1998; Claxton, et al., 1999). These guidelines include recommendations for sump designs, where critical dimensions are normalized with the suction bell inlet diameter, such as: clearances between the suction bell and floor-side walls, sump width-length, baffles, and corner fillers. Additional recommendations are provided for operational parameters, such as minimum submergence, and velocity of the approach inflow across the sump and at the bell inlet.

Model Study of Pump and Sump

The above guidelines also provide criteria for physical model studies covering:

- Need for model
- Objectives (flow pattern at impeller eye)
- Similitude and scale selection
- Scope, i.e., boundary including a “sufficient area of the approach geometry” (upstream suction system)
- Instrumentation, and measuring techniques and parameters
- Acceptance criteria (type of vortices, value and steadiness of swirl angle value, time-average and fluctuations of the axial velocity pattern at suction bell throat corresponding to the impeller eye)

The primary attention for the model test is on the formation of vortices (Daggett and Keulegan, 1974; Hecker, 1981; ANSI/HI 9.8, 1998). Therefore, the Froude number similarity is adopted for the model test ($Fr_m = Fr_f$, m-model and f-full), where the scale model factor is selected on the basis of model data extension to full size, model measurement accuracy, and model cost.

If the fluid is the same for the model and the site (usually clean water for the model), the Froude similarity excludes the Reynolds similarity (being $Re_m / Re_f = L_r \times 1.5$, $L_r = \text{geometrical scale factor}$) (Blevins, 1984). Although some criteria regarding the minimum value of Re_m are applied to ensure full turbulent flow conditions in the model, some questions may arise about the

extension of the flow model simulations and the correlation with site flow patterns (Padmanabhan and Hecker, 1984).

In essence, the suction system (intake and sumps) should be designed with the objective to produce a relatively uniform and steady velocity distribution at the pump bell throat (impeller eye). This flow pattern will occur:

“if the flow enters the bell essentially radially, without pre-swirl or local low disturbances such as vortices or eddies caused by local low separation. Therefore, all of the above ... [steps], starting with providing a uniform approach flow [from the intake] ... may be needed to achieve the desired uniformity of velocities” (ANSI/HI 9.8, 1998).

This identical statement is formulated in other reference publications (Dicmas, 1987; Karassik, et al., 2001) as distillation of the experience with many field problems (Gatz, 1999).

Circulation Pumps—Mixed-Flow Vertical Turbine Configuration

Vertical turbine pumps are widely used for cooling water system wet-pit installation (open sumps). The pump cross-section shown in Figure 1 is a sketch of the pump discussed in this paper. This pump configuration is typical of thousands of vertical turbine pump installations for many pumping services and various pump manufacturers.

Vertical turbine pumps, such as these, usually use mixed-flow impellers. A comparison of various impeller designs (centrifugal, mixed-flow, and axial-flow) with their corresponding specific speeds (N_s) is shown in Figure 2 (Karassik, et al., 2001). Specific speed is an index number correlating pump flow, head, and speed at the optimum efficiency point.

The specific speed (N_s) is defined by:

$$N_s = \frac{N\sqrt{Q}}{H^{0.75}} \tag{1}$$

where:

- N = Speed, rpm
- Q = Flowrate (gpm) at BEP
- H = Head, ft

A peculiar characteristic of all vertical turbine pumps, or bowl diffuser pumps, is the meridional configuration of the impeller with “diagonal” shape having a semiaxial discharge (blade trailing edge), which is the reason for the name “mixed-flow” for such pumps. This mixed-flow aspect is not strictly related to specific speed (e.g., it is present for moderate N_s like 1800 to 2500, which tend to be classified as “centrifugal flow pumps,” which have a fully radial impeller discharge). Then the name “diagonal impeller” is more indicative. The inclination of the exit impeller edge increases with specific speed becoming more “axial.”

Determining Suction Recirculation Onset Capacity

There is a peculiar effect on the shape of the performance curves at part flow below BEP (i.e., the presence of an inflection point or region on the power and head curves). With specific reference to the head curve, the inflection point may be associated with zero slope of the flow-capacity curve, or even a dip in the curve (depending on specific speed and also impeller design) for $N_s = 4000$ to 7000 . Another peculiar aspect is that below such flow point (region), the head curve rises very rapidly. This aspect is not fully evident with “centrifugal flow pumps” (i.e., impellers with radial discharge even for $N_s = 3000$ to 5000), which would be considered as “mixed-flow.”

The physical phenomenon behind such peculiar aspects of power and head curve is the occurrence of discharge and suction recirculation, which has been experimentally proven by different methods including:

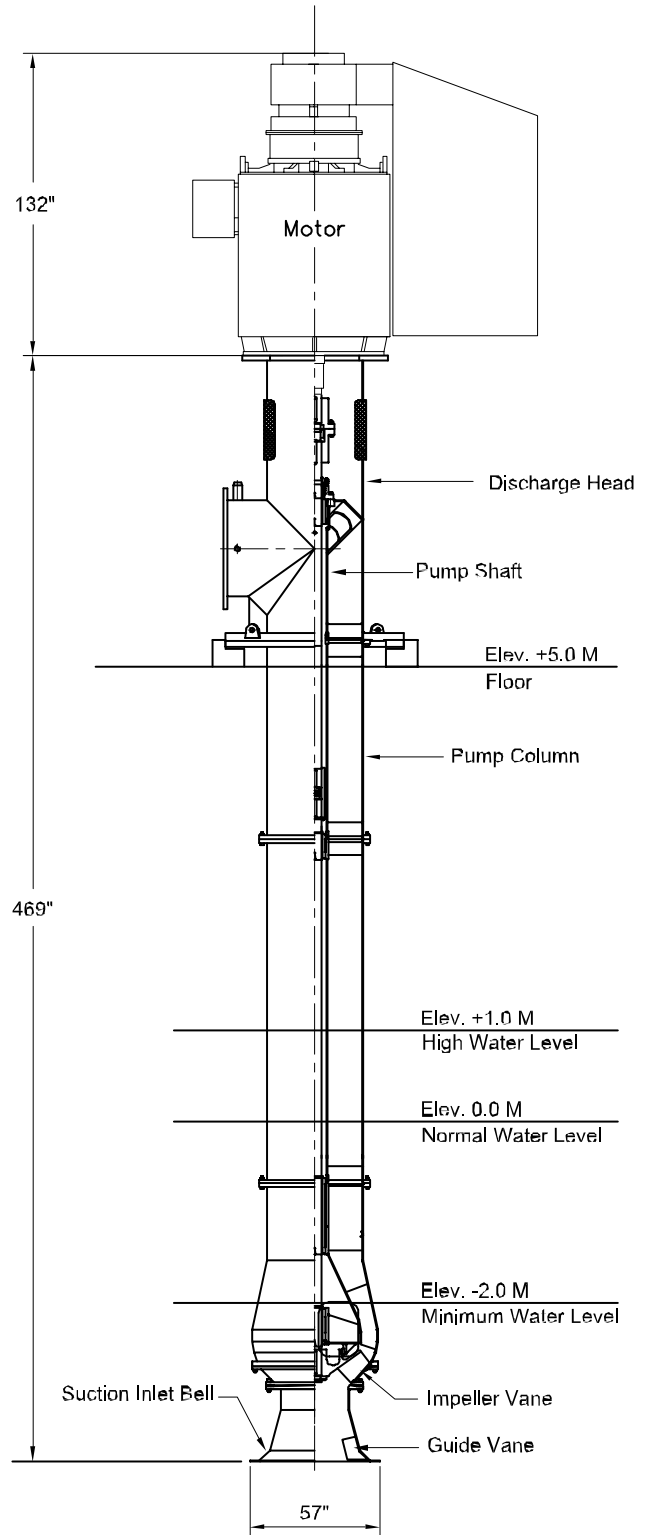


Figure 1. Cross-Section of Vertical Turbine Pump.

- Flow visualizations (Murakami and Heya, 1966; Toyokura and Kubota, 1968, 1969)
- Statistical analysis of performance (Rey, et al., 1982)
- Static pressure measurements plus flow traverses (Schiavello and Sen, 1980, Schiavello, 1982)
- Minitransducers for dynamic pressure installed directly on the impeller (Kauptert and Staubli, 1999a, 1999b)

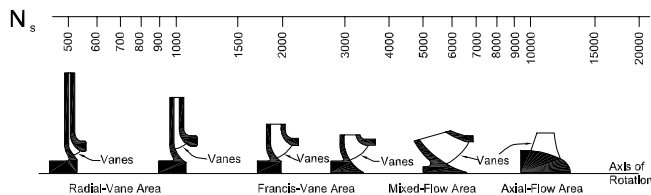


Figure 2. Approximate Range of Specific Speeds for Various Impeller Types.

It can be inferred that the analysis of the shape of power and head curves from shop tests can provide insights regarding the onset of suction/discharge recirculation for vertical turbine pumps with diagonal impellers. These changes in the performance curves are more evident than for centrifugal flow pumps of identical specific speed and suction specific speed (N_{ss}). Suction specific speed is calculated by the same formula as pump specific speed, but uses NPSHR values instead of head (H).

The suction specific speed is defined by:

$$N_{ss} = \frac{N\sqrt{Q}}{NPSHR^{0.75}} \quad (2)$$

where:

N = Pump speed (rpm)

Q = Flowrate (gpm) at BEP

NPSHR = Net positive suction head required to prevent cavitation at BEP

Also, the aspects (onset/intensity) of suction recirculation for centrifugal pumps with radial outlet impellers (e.g., volute pumps) are different compared to pumps with mixed-flow diagonal outlet impellers for the same N_s . This basically means that “global” type information used to evaluate the potential for suction recirculation, such as: suction recirculation versus suction energy (Budris, 1993; ANSI-HI, 9.6.1, 1998), empirical prediction correlation (Fraser, 1981), and field statistical correlations of suction recirculation versus N_{ss} (Hallam, 1982), are not likely applicable to vertical turbine pumps because their background basis is from centrifugal flow pumps.

Suction Recirculation—Nature, Key Aspects, Influence of Upstream Flow Pattern

It has been recognized since the mid 1970s (Bush, et al., 1975, 1976) that operating pumps at reduced flows can generate harmful effects, such as high pressure pulsation, vibration, noise, and unsteady dynamic loads. Experimental investigations with centrifugal flow pumps using both flow visualizations (Minami, et al., 1960) and internal flow measurements (Ferrini, 1974; Schiavello, 1975; Sen, 1976) have clearly shown that when the capacity is reduced below the best efficiency point, a complex three-dimensional flow pattern suddenly appears at the impeller inlet.

This flow pattern is induced from the impeller itself and is characterized by:

- Flow reversal at the eye of the impeller (i.e., negative axial velocity component) also called “backflow”
- A vortex with tangential velocity swirling at the rotational speed also called “prerotation”
- Radial static pressure distribution with higher value at the outer periphery (suction pipe wall)

Actually, these phenomena are common to all pump types including: horizontal and vertical, single and multistage, centrifugal-flow (Minami, et al., 1960; Janigro and Schiavello, 1978), mixed-flow (Murakami and Heya, 1966; Toyokura and

Kubota, 1969; Massey, 1976), axial-flow (Toyokura and Kubota, 1968), and inducer.

Since the early 1980s, the name “suction recirculation” has become almost synonymous when referring to this complex flow pattern. The flowrate at which it appears at the impeller inlet is commonly referred to as the “suction recirculation capacity.” A key observation is that the appearance of suction recirculation is characterized by a sudden rise of the static pressure at the pipe (or casing) wall in front of the impeller, which led to the development of a simple detection method (Schiavello, 1975; Schiavello and Sen, 1980).

A peculiar characteristic was visually observed by Schiavello (1975, 1978) using a mercury multimanometer connected to an angular distribution of pressure taps around the pipe wall near the impeller inlet and confirmed by Sen (1976, 1978). An unsteady flow pattern first shows up at onset, which persists for a narrow capacity window and is followed by a steady swirling annular flow in the presence of steady uniform incoming flow after a small reduction of the capacity.

Chauvin, et al. (1980), made the hypothesis that this unsteady phenomenon has a close analogy with rotating stall in compressors. Direct quantitative measurements were performed by Sen, et al. (1979), which determined both the amplitude and the frequency of this “unsteady flow” revealing a periodic character with a dominant subsynchronous frequency near 30 percent of rotating speed and confirming the nature of the rotating stall.

The onset of suction recirculation can also be detected by observing suction pressure gauge fluctuations (Fraser, 1981). The amplitudes and the frequency spectra of the pulsation can be determined more accurately using dynamic pressure transducers installed near the impeller eye (Breugelmans and Sen, 1982). This experimental method was also used by Sloteman, et al. (1984), to obtain data under cavitating conditions.

These measurements indicated that suction recirculation creates large-scale turbulence and low-intensity broadband pressure fluctuations over a large frequency range from 1 Hz to 2000 Hz. These pressure pulsations can excite acoustic natural frequencies of the suction/discharge piping system that can result in high vibration levels (Schiavello, 1988), mechanical natural frequencies of the pump rotor, the pump housing, the motor, and the piping (Sulzer Pumps, 1998), and surge of the suction system (Massey, 1976). Dynamic pressure transducers were installed at the impeller inlet in the field case discussed in this paper.

A common physical triggering mechanism for centrifugal-, mixed-, and axial-flow pumps has been suggested by Schiavello (1975) and Schiavello and Sen (1980). When the capacity is decreased, the incoming flow reaches a high positive incidence angle, which causes a high blade loading on the suction side of the blade tip at, or near, the leading edge. At a certain capacity, the limiting stalling incidence is reached and local separation begins (characteristic of rotating stall). As the flowrate is further reduced and the back (discharge) pressure is increased, a reverse flow arises immediately that forces prerotation through shear stresses. Therefore, two crucial impeller design parameters are:

- The incidence angle of the blade tip at the impeller inlet, and
- The loading at the vane tip and its span-wise load distribution from the hub-to-tip (Schiavello and Sen, 1980).

With reference to the prediction of the suction recirculation onset capacity, an approach based on diffusion factor has been discussed by Schiavello and Sen (1980) and Schiavello (1983), which in principle could be applied to all pumps (using the same parameters to predict stalls in subsonic centrifugal compressors). Moreover, an empirical correlation using some impeller geometrical parameters has been published by Fraser (1981), which has been derived from a large database of centrifugal flow pumps (Fraser, 1983). A discussion dealing with various prediction approaches was also presented by Schiavello (1982) based upon a comparison with experimental data.

Overall trends of suction recirculation onset capacity and intensity (effects) with global parameters, such as suction specific speed, based on gross field statistics (Hallam, 1982) are just qualitative with high-scatter. These generalizations can even be misleading, especially, if they are applied to modern design pumps where blade geometries are optimized to achieve low NPSHR that result in high Nss values (Schiavello, 1993). Certainly, old impeller design methods relying only on large-eye impellers with shockless capacity well above the BEP for achieving high Nss are prone to bad suction recirculation behavior. Therefore, field statistics including such old impeller designs cannot be generalized and used to evaluate new impeller designs.

The utmost influence of the upstream flow pattern on the onset and development of suction recirculation was experimentally determined. The suction recirculation onset capacity is moved to lower capacity if the impeller inlet is progressively throttled with orifice plates in a way to produce a shockless (zero incidence) condition at each flowrate (Murakami and Heya 1969), and a partial asymmetric blockage in front of the impeller causing flow distortion increases the onset capacity according to internal data (unpublished). Moreover, experiments with subsonic flow compressors have shown that the stall line is moved to higher flow, if a flow distortion (asymmetric blockage) is forced at the compressor inlet (Colpin, 1977).

Discharge System

The discharge system is basically formed by all the components downstream of the pump bowl. The system can interact or respond (structurally and/or acoustically) to the unsteady flow patterns occurring inside the pump components (bell-impeller-bowls), which act as exciting sources.

The major components of the discharge system include the pump column, the pump shaft, the discharge head, and the motor (Figure 1). Additional major components include the discharge piping system from the pump discharge flange to the condenser inlet box (i.e., expansion joint, throttle valve, check valve, piping characteristics: length, diameter, wall thickness, etc.).

FIELD VIBRATION PROBLEM

Three large high-energy vertical pumps operated satisfactorily with acceptable vibration levels during factory acceptance tests but experienced excessive vibration and noise problems when installed at the site. The normalized shop test performance curves are shown in Figure 3. Vibrations measured at the top of the motor during the shop tests are shown in Figure 4.

At the site, one pump could operate satisfactorily with low vibration levels. However, the vibration and noise levels increased significantly when two pumps were operated in parallel, or when one pump was operated at reduced flowrates by throttling discharge valves. These problems were unusual because the excessive vibration levels occurred at flowrates above the BEP.

The vertical pumps were installed in parallel to provide cooling water (“circ water”) for a power plant (Figure 5). The circulating water system can operate with one or two pumps in service. During normal operation, two pumps are in service with the third pump as a spare. The system design flowrates are 65,300 gpm (14,831 m³/hr) with one pump in service, and 56,000 gpm (12,719 m³/hr) per pump with two pumps in service. As shown in Figure 6, both these flowrates are above the pump BEP value.

The flowrates are not metered at the site; therefore, the flowrates were computed based upon measured pressures, head, and power levels. The discharge pressures were approximately 3.2 bar (46.4 psi) during single pump operation and 3.6 bar (52.2 psi) during two-pump operation. The specifications for the pump and motor are shown in Table 1. The pump specific speed is 3150, which is considered to give high efficiency. The pump suction specific speed is 10,600.

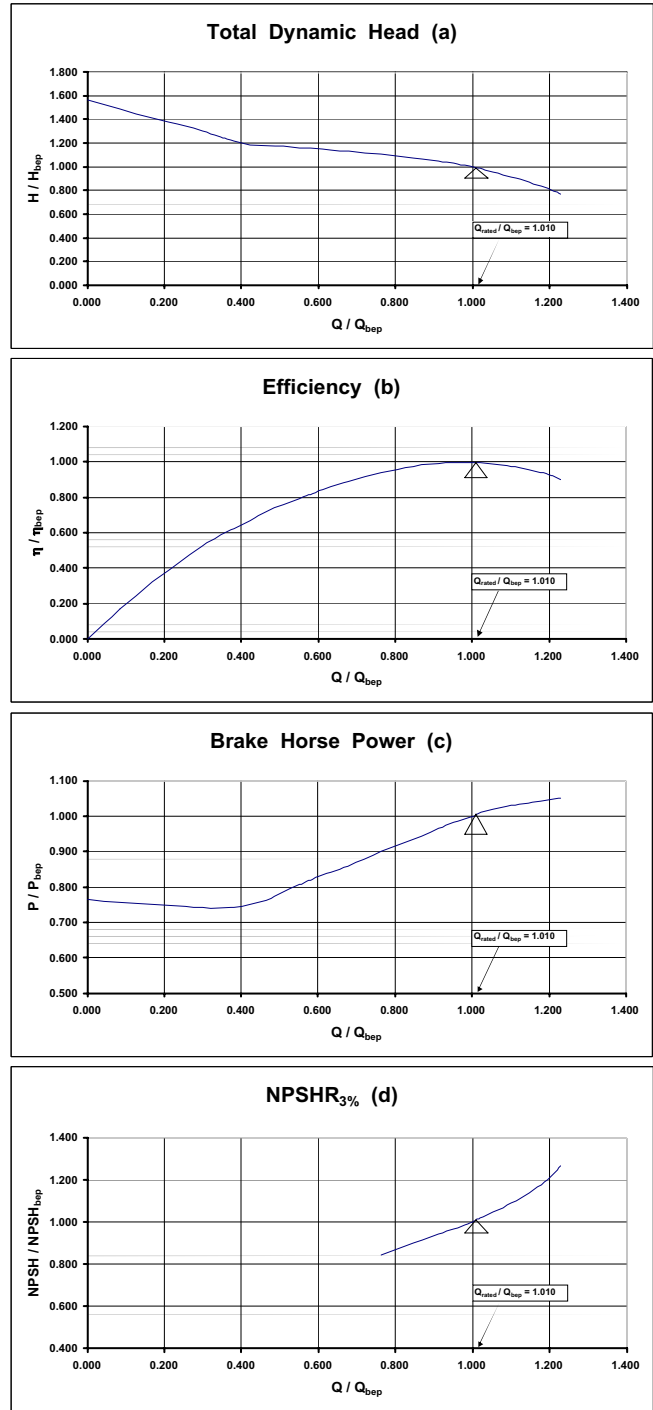


Figure 3. Normalized Shop Performance Curves.

As shown in Figure 7, seawater is pumped through an inlet pipe, which connects to a common header on the side of the intake structure where the pumps are installed in three separate cells (Figures 8 and 9). Three 78 inch diameter pipes supply the water to the three cells.

The three pumps discharge into a common header. The water is pumped approximately 400 meters (1312 ft) to the condenser at the power plant at an elevation of approximately 31 meters (102 ft) above sea level. After leaving the condenser, the water flows through a “drop structure” and back to the sea.

Prior to construction, hydraulic model studies were made of the pump intake structure by an independent lab. These model studies are described in greater detail later in the paper. The scale model

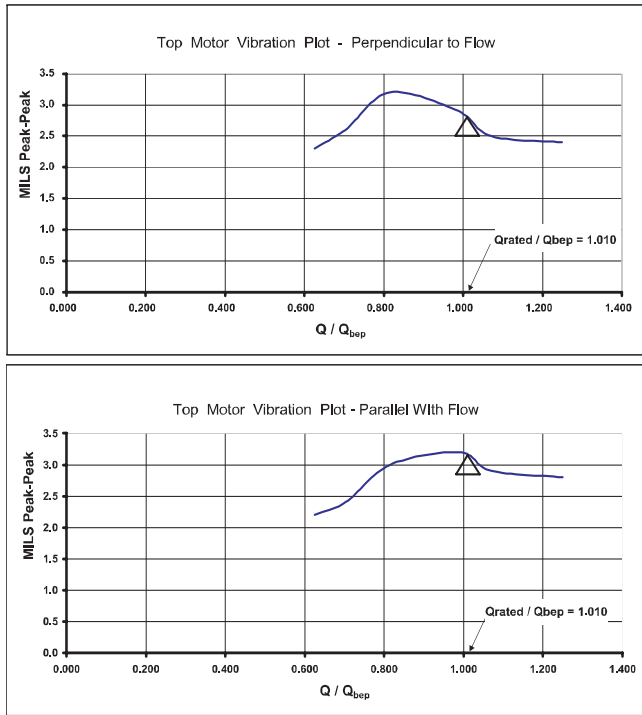


Figure 4. Motor Vibration During Shop Performance Tests.



Figure 5. Photograph of Pump Installation at Power Plant.

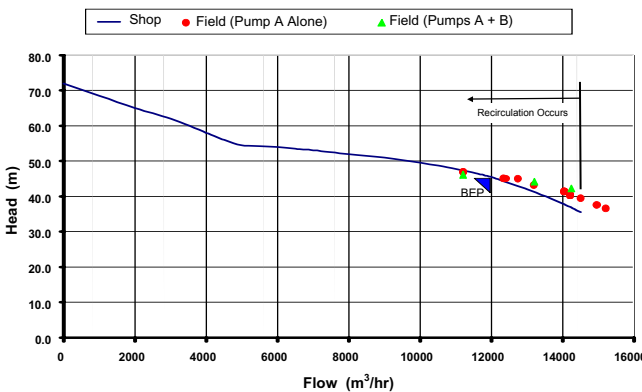


Figure 6. Operating Conditions in Field Versus Shop Test.

included the three pump cells (bays), the auxiliary cooling water pump located in one bay, and the major structural features likely to affect flow through the pump intake structure.

Table 1. Pump and Motor Specifications.

Item	Value
Pump Application	Circulating Water Pump
Pump Size	56" Bowl Diameter
Pump Rating at BEP	52,500 gpm (11,924 m ³ /hr) at 585 rpm
Total Head	150 ft (45.72 m)
Number of Stages	One
Impeller	Open Impeller with 7 blades, Bowl
Fluid Specific Gravity	1.03 (seawater)
Pump Specific Speed, Ns	3150
Suction Specific Speed, Nss	10,600
Driver	Induction Motor – Frame Size V8014
Power	2650 hp (1976 kW) at 597 rpm

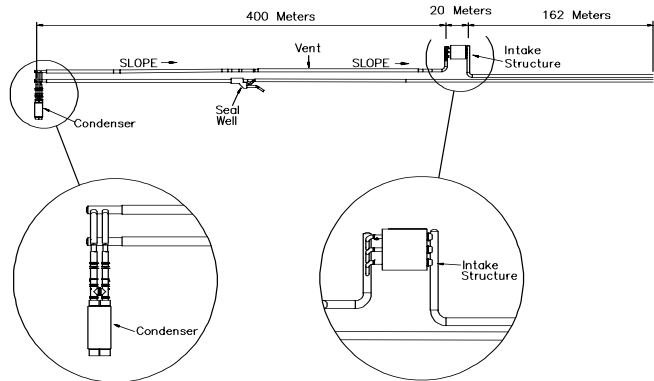


Figure 7. Layout of Cooling Water System.

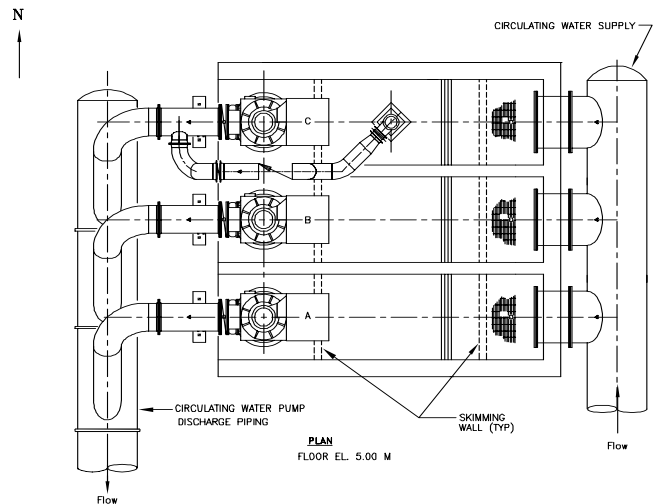


Figure 8. Sketch of Water Intake Structure—Plan View.

The objectives of the hydraulic study were to verify the absence of undesired flow patterns/phenomena (ANSI/HI 9.8, 1998) and, if necessary, modify the design of the pump intake structure. These studies indicated several undesirable flow conditions such as vortices, flow separations, asymmetry in the approaching flow, etc. Several modifications were made to eliminate the undesirable flow conditions at the pump bell. These modifications included: shortening the bay, setting the pump bell approximately 0.5 m (1.6 ft) from the floor, adding a curtain wall between the inlet pipe and the trash rack, adding a second curtain wall near the pump, adding fillets at the wall-floor corners, and adding a flow splitter under the pump bell (Figures 8 and 9).

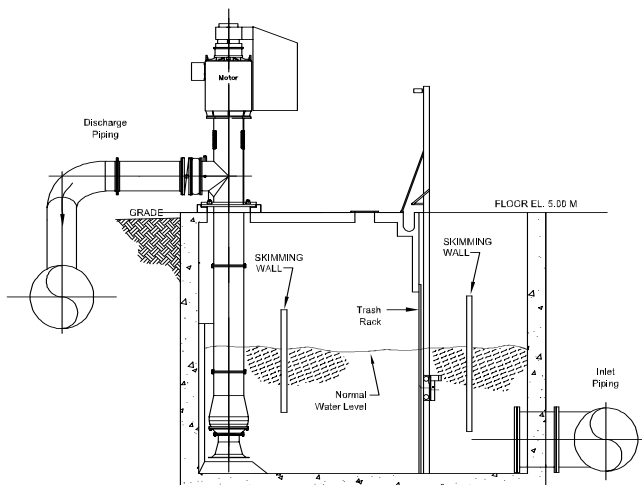


Figure 9. Sketch of Water Intake Structure—Elevation View.

Description of Problems

Each pump performed satisfactorily when operated alone at flowrates well above the BEP. However, the vibration and noise levels significantly increased when two pumps were operated together at flowrates below 120 percent BEP, or when a single pump was operated alone at similar flowrates.

During operation with two pumps, the discharge pressure increased while flow per pump decreased, leading to strong vibrations of the pump and motor, which became even more violent when the pump operating point was lowered below the BEP. These problems were identified during the commissioning of the pumps. The vibration and noise levels were considered to be excessive for long-term operation. The maximum vibration levels occurred on the top of the motors and were visible to the naked eye. The high motor vibration resulted in damage to the coolers mounted on the motors. One of the pumps experienced a lower bearing failure that could have been related to the excessive pump vibration.

The high level “roaring” type noise was also characterized by a metal against metal rattling sound that was thought to be caused by the unshrouded impeller vanes contacting the bowl front wall. The roaring or rumbling type noise is an indication of operating the pump away from the preferred range of operation (Karassik, 1981). The noise was not the classical cavitation sound that is often described as a cracking sound similar to “pumping rocks in the pipe.”

Furthermore, vibration of the condenser (which was approximately 400 meters [1312 ft] away) also increased when the vibration and noise increased at the pumps. Failures of condenser tubes had also occurred that might have been caused in part by this vibration.

Initially, it was thought that these problems were associated with some phenomenon peculiar to two-pump operation. However, this hypothesis was disproved since a single pump operating with increased head pressure also experienced the same problems. Therefore, it was hypothesized that the operation at higher head pressures (lower flowrates) caused the problems to occur.

Initial analyses of the vibration data indicated that the excessive vibration occurred at nonsynchronous frequencies with the major amplitudes at a response near 11 Hz. The vibration levels at the running speed were very low. The vibration levels at the top of the motor and the pump housing were well above the levels specified by the Hydraulic Institute for vertical pumps (ANSI/HI 2.1-2.5, 1994) and the pump manufacturer.

In an effort to reduce the excessive vibration levels of the pumps and motors, structural braces were installed to the top of the pump. As shown in Figure 10, diagonal steel beams were added between the pump head and the concrete mat. Additional steel beams were installed to tie the three pumps together, and to attach pump C to the adjacent building. Although these braces reduced the vibration

levels, the vibration frequency did not change and the levels were still considered to be excessive, which indicated that there were high-level forces acting on the pump/piping system. Also, since the braces were not intended to reduce pulsation, the condenser vibrations were not reduced.

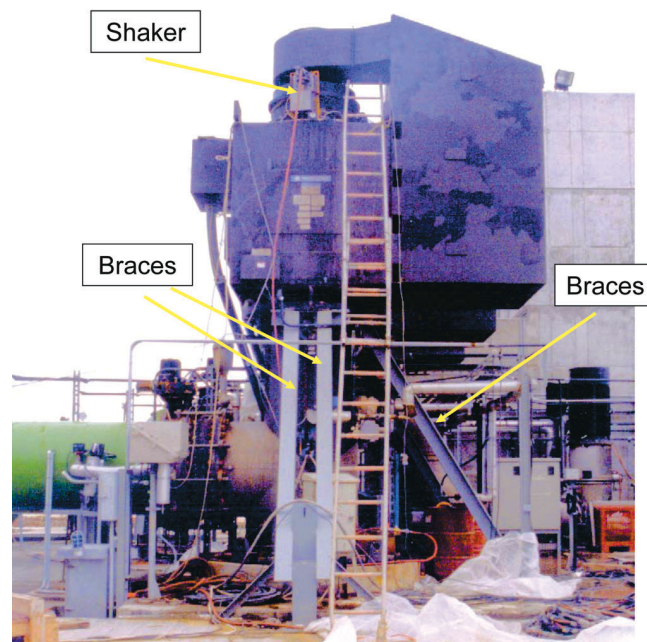


Figure 10. Diagonal Braces Added to Reduce Vibration Levels.

A preliminary root cause analysis meeting between the pump manufacturer, the design company, the engineering and construction company, and initial consultants developed the following hypotheses.

- *Air leakage into pump*—Initially, it was thought that the problems were due to entrained air caused by air leakage into the pump inlet.
- *Excitation of mechanical natural frequencies*—The vibrations could be amplified by the excitation of the pump’s mechanical natural frequencies.
- *Inlet flow disturbances*—Some weak surface vortices were observed on the water surface in the bays near the pumps.
- *Excitation of acoustic natural frequencies*—The pulsations in the system could be amplified by the excitation of the pump/piping system acoustic natural frequencies.

First Field Test

Field data were obtained to assist with the root cause analysis. The primary objectives of these tests were:

- Determine the major causes for the excessive vibration on the pumps when two pumps were in service
- Determine the cause(s) of increased vibration at the condenser inlet piping during two-pump operation
- Determine if the problems could be attributed to a single component (such as an improperly designed pump), or was the situation related to the entire system (such as acoustical resonances, structural resonances, etc.)

Shaker Tests

Shaker tests were conducted on pump A to measure the mechanical natural frequencies of the pump/motor system. The pump was tested with and without the diagonal braces, and with a wet and dry sump configuration.

A variable speed mechanical shaker was attached to the top of the motor as shown in Figures 11 and 12. The shaker was driven by a variable speed air motor over a speed range from approximately 150 to 1000 rpm. The shaker was oriented with the shaft in the vertical position such that the rotating shaking forces were in the same direction as an imbalance on the motor/pump shafts. During these tests, the shaker unbalance was set to 48.8 lb-in. This unbalance would be approximately 10 times larger than the typical API allowable residual unbalance for the motor and pump rotors operating at 600 rpm.

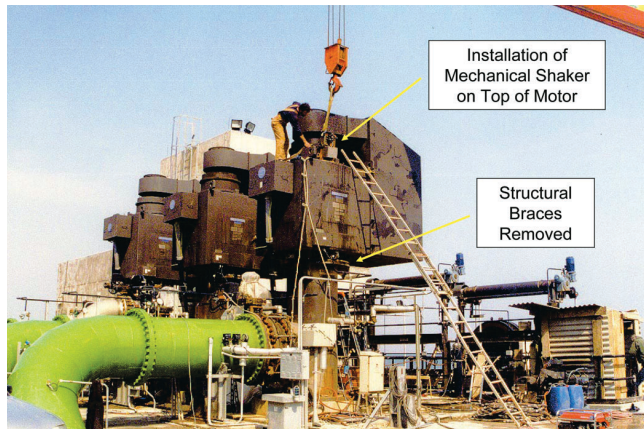


Figure 11. Installation of Mechanical Shaker on Top of Motor.

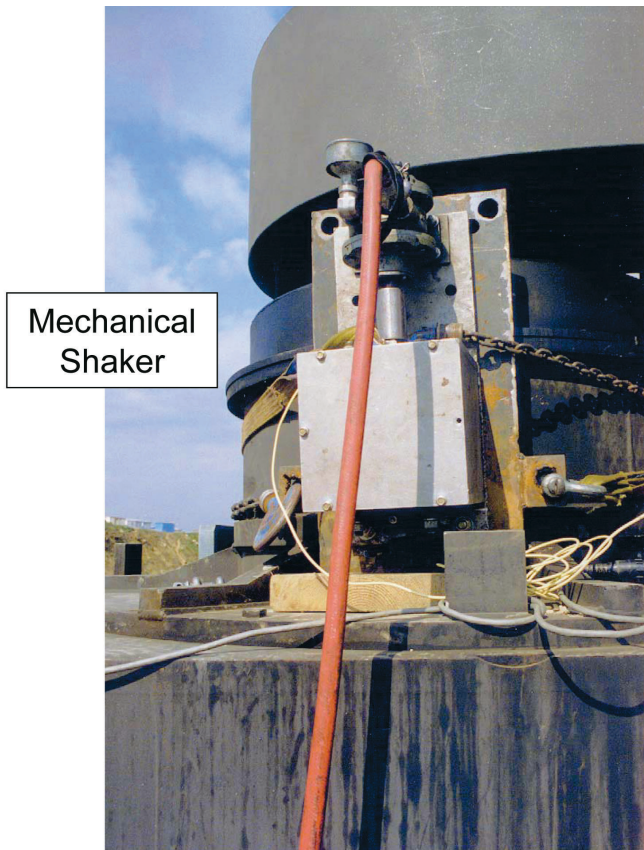


Figure 12. Closeup View of Mechanical Shaker Attached to Motor.

The pump and motor vibrations were measured using accelerometers. Single-axis accelerometers were magnetically attached to the top of the motor in the E-W and N-S directions. The accelerometers were located near the vertical centerline of the motor, inline with

the shaft. Accelerometers were also installed at the top of the pump housing (Figure 13). A waterproof triaxial accelerometer was installed on the pump inlet bell to measure the vibrations of the pump column (Figure 14). The acceleration signals were double-integrated to obtain displacements in mils (0.001 inches).

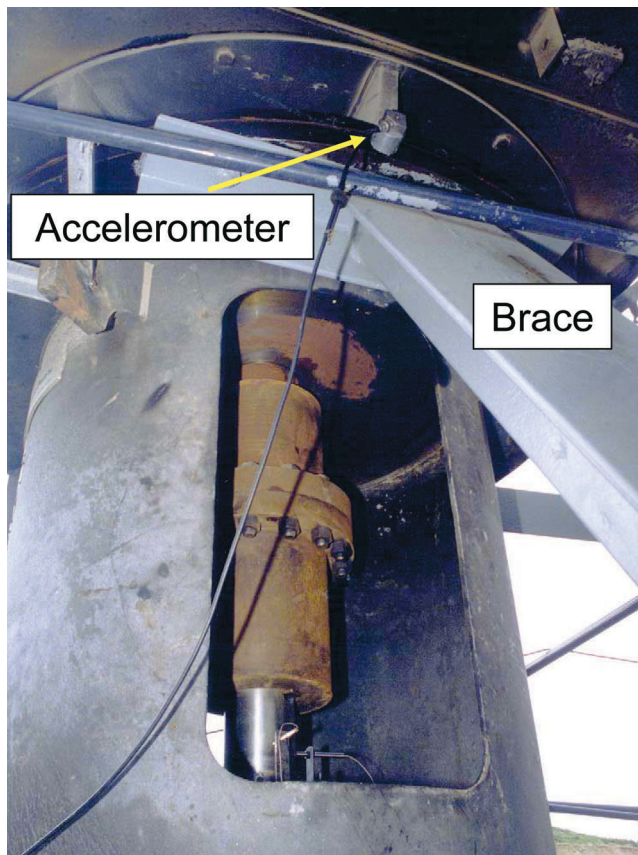


Figure 13. Accelerometer Location at Top of Pump Housing.

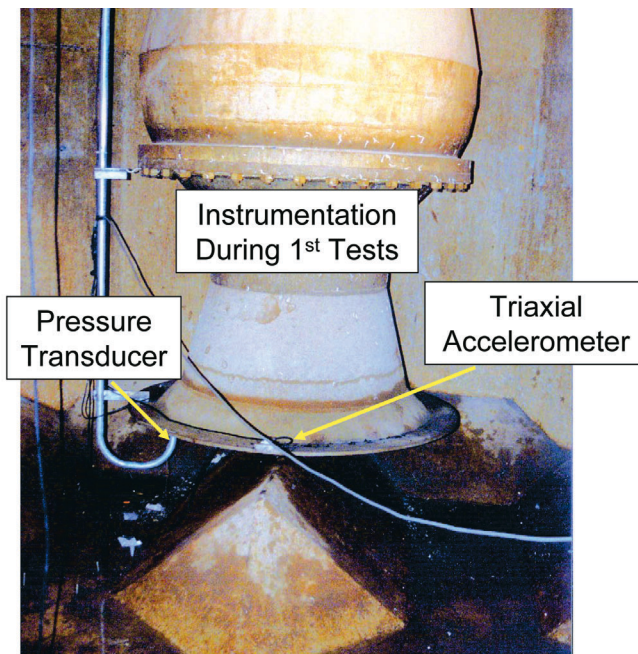


Figure 14. Pressure Transducer and Accelerometer Installed on Pump Suction Bell.

Pump shaft vibrations relative to the pump housing were measured using proximity probes mounted near the coupling (Figure 15).

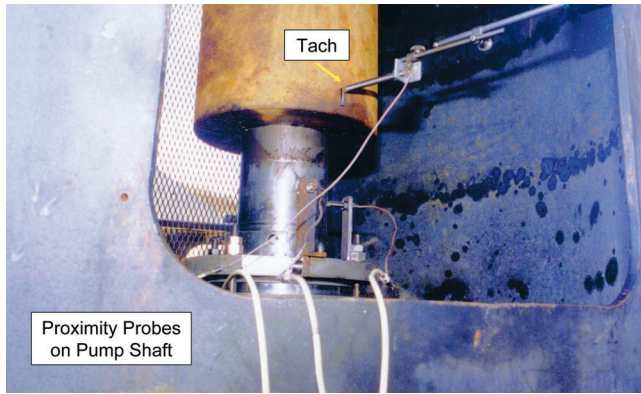


Figure 15. Proximity Probes Installed at Top of Pump Shaft (Near Coupling).

The mechanical natural frequencies were easily identified from the shaker test data. Typical plots of the vibrations at the pump inlet and the top of the motor are given in Figures 16 and 17. The measured natural frequencies were obtained during the tests with the sump filled with water and with all the braces removed. The directions refer to the flow direction out of the discharge pipe. The parallel direction is in the E-W direction, and the perpendicular direction is in the N-S direction. As shown in Table 2, the major responses had very high amplification factors.

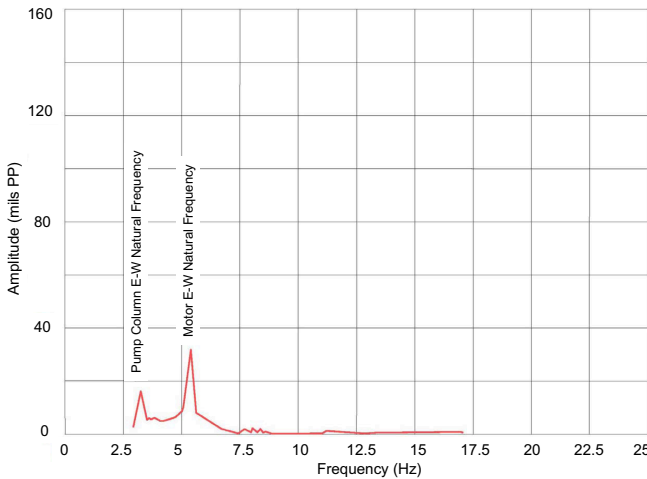


Figure 16. Vibration Responses of Pump Inlet in E-W Direction Due to Shaker (Sump Filled and All Braces Removed).

The motor natural frequency at 11 Hz was a twisting mode about the vertical axis. The vibration levels at the outer corners of the motor housing were approximately three times higher than the amplitudes measured at the motor centerline.

Additional shaker tests with the diagonal braces installed showed that the braces shifted the 11 Hz mechanical natural frequency slightly, but the vibration amplitudes were unaffected because the braces did not reduce the twisting motion of the motor. This behavior explains why the braces did not eliminate the vibration near 11 Hz.

Operating Tests

Previous tests had indicated that the vibration and noise levels were satisfactory with one pump operating and significantly

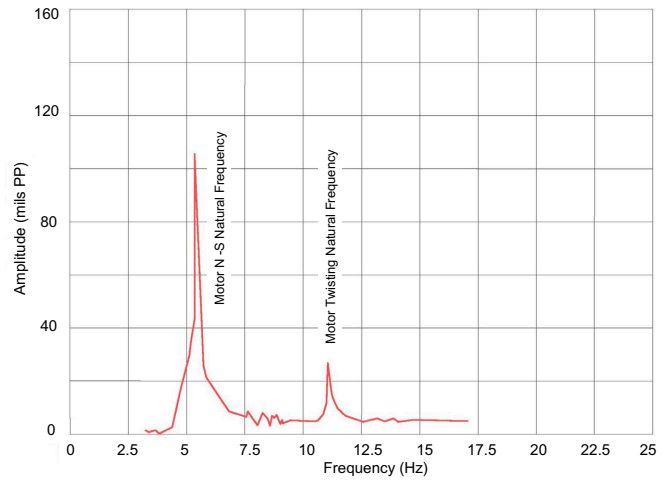


Figure 17. Vibration Responses of Top of Motor in N-S Direction Due to Shaker (Sump Filled and All Braces Removed).

Table 2. Measured Pump/Motor Mechanical Natural Frequencies.

Direction	Frequency	
Pump Column N-S (perpendicular)	2.8 Hz	170 cpm
Pump Column E-W (parallel)	3.25 Hz	195 cpm
Motor E-W (parallel)	5.25 Hz	315 cpm
Motor N-S (perpendicular)	5.36 Hz	322 cpm
Motor (twisting)	~11 Hz	650 cpm

increased with two-pump operation. The high vibration and noise levels could also be duplicated during single-pump operation when the discharge pressures were increased by throttling a discharge valve at the pump or at the condenser. A test plan was devised to obtain vibration and pulsation data at several locations throughout the pump/piping system during various operating conditions. Vibration could then be compared to pulsation to evaluate causality. A sufficient number of pulsation transducers were installed to determine if pulsation was localized, or if it had systemwide response characteristics.

Instrumentation—Vibration was measured with accelerometers installed on the motor, the pump, and the condenser. Pulsation data were obtained using piezoelectric dynamic pressure transducers. These pressure transducers were installed in the following locations:

- *Pump discharge flange*—Test point in the pump discharge head just before the pump flange (Figure 18)

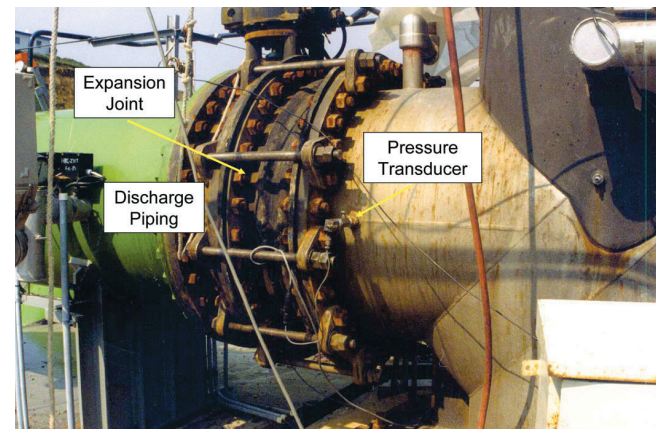


Figure 18. Pump Discharge Elbow Showing Expansion Joint and Pressure Transducer Location.

- *Standpipe*—Test point at the base of the standpipe (vent). This point was near the midpoint of the discharge piping between the pumps and the condenser (Figure 7).

- *Pump inlet*—Test point at the pump inlet bell. A waterproof dynamic pressure transducer was not available; therefore, an attempt was made to obtain pulsation data using a normal, nonwaterproof transducer. A dynamic pressure transducer and a charge amplifier were installed inside a section of conduit that was secured to the pump inlet bell (Figure 15). Some data were obtained with this pressure transducer until it eventually failed due to water leaking into the conduit.

- *Pump sump*—Additional pulsation data were obtained in the sump away from the pump using another nonwaterproof pressure transducer that also installed in a section of conduit.

Static pressure data were obtained using variable reluctance pressure transducers. These transducers measure both the static pressure and dynamic pulsation. These transducers were installed at the following locations.

- *Pump discharge flange*—Test point in the pump discharge head just before the pump flange (Figure 19)

- *Condenser*—Inlet piping just before the condenser

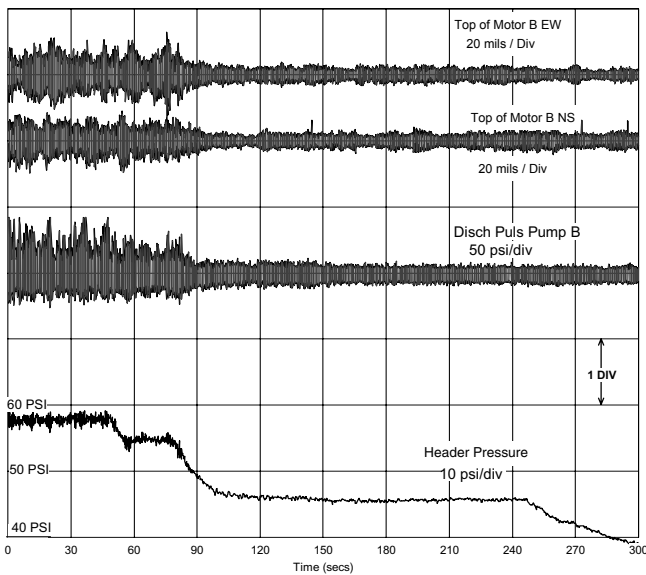


Figure 19. Vibration at Top of Motor and Discharge Pulsation During Throttling Test of Condenser Outlet Valves as Discharge Pressure was Reduced from 3.9 to 2.6 Bar (56.5 to 37.7 PSI).

Test Results

Data were obtained in two-pump service with various pump combinations, and with the pumps operating individually with throttling at the pump discharge block valve or at the butterfly valve downstream of the condenser. During the throttle tests, the pump discharge valve or the valve downstream of the condenser was slowly closed, which increased the discharge pressure and reduced the flowrate. The test data indicated that when the discharge pressure was increased, there was a “threshold” pressure where the pulsation and vibration levels suddenly increased. Similarly, the vibration and pulsation levels were suddenly reduced when the valve was opened and the discharge pressure was lowered below the “threshold” pressure.

Data obtained on pump B during throttling tests as the butterfly valve downstream of the condenser was slowly opened are shown in Figures 19 to 24. A sudden reduction in the vibration and discharge pulsation occurred as the discharge pressure was reduced below 47 psi (3.24 bar) (Figure 19).

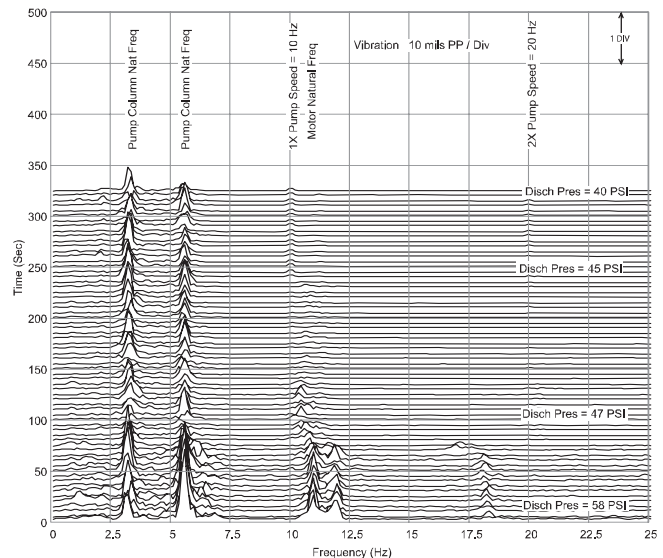


Figure 20. Frequency Spectra of Motor Vibration in N-S Direction During Throttling Test of Condenser Outlet Valves as Discharge Pressure was Reduced from 3.9 to 2.6 Bar (56.5 to 37.7 PSI).

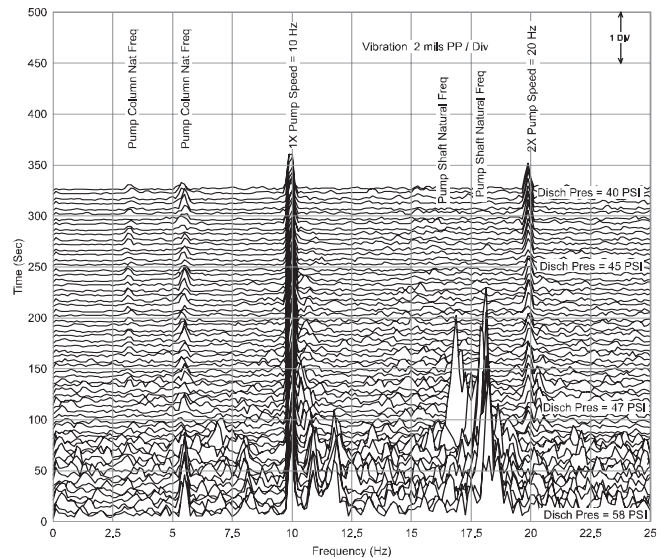


Figure 21. Pump Shaft Vibration Near Coupling During Throttling Test of Condenser Outlet Valves as Discharge Pressure was Reduced from 3.9 to 2.6 Bar (56.5 to 37.7 PSI).

When the pump was operating at a discharge pressure above 3.2 bar (46.4 psi), an increase in broadband energy occurred that excited the mechanical natural frequencies of the pump/motor system, the lateral natural frequency of the pump rotor, and the acoustic natural frequencies of the pump/piping system.

Motor vibration occurred primarily at 3.3 Hz, 5.5 Hz, and 10.75 Hz (Figure 20). These frequencies matched the mechanical natural frequencies that were measured during the shaker tests. Pump shaft vibration near 17 to 18 Hz was thought to be the lateral natural frequency of the pump shaft (Figure 21).

Pulsation near 11 to 12 Hz (Figure 22) was due to excitation of one of the acoustic natural frequencies of the pump/piping system. Pulsations at this acoustic natural frequency were measured at the pump discharge, in the standpipe, and at the condenser, and were consistent with the acoustical mode shapes predicted for this system. Additionally, pulsation at the condenser at 11 Hz (Figure 23) appeared to excite the mechanical natural frequency of the condenser (Figure 24).

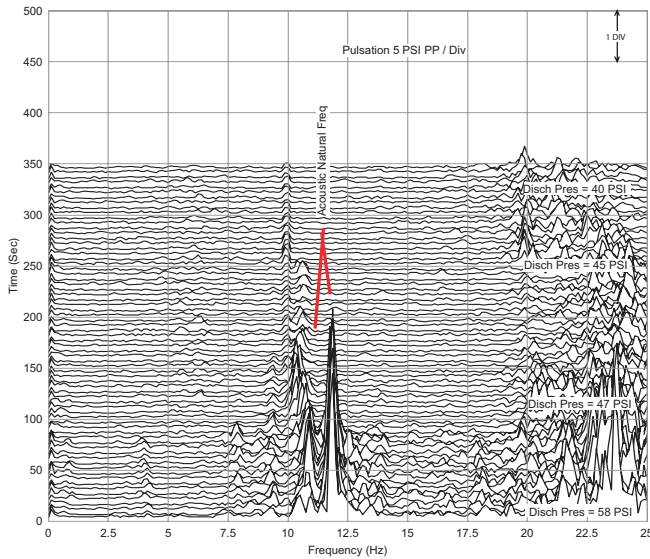


Figure 22. Pump Discharge Pulsation During Throttling Test of Condenser Outlet Valves as Discharge Pressure was Reduced from 3.9 to 2.6 Bar (56.5 to 37.7 PSI).

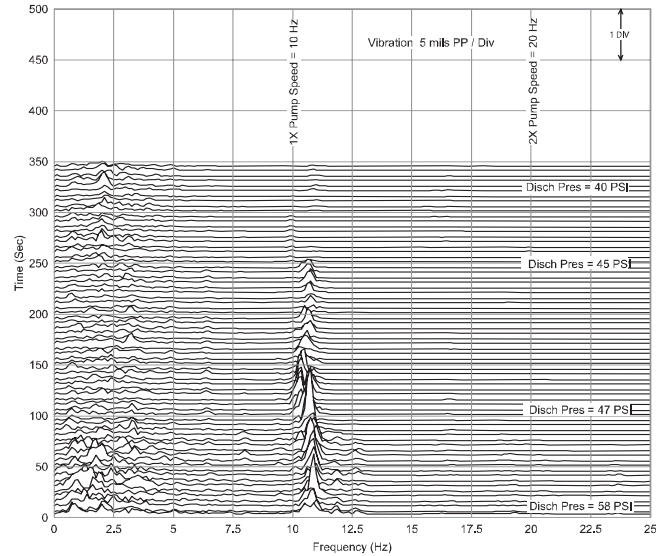


Figure 24. Vibration at Condenser During Throttling Test of Condenser Outlet Valves as Discharge Pressure was Reduced from 3.9 to 2.6 Bar (56.5 to 37.7 PSI).

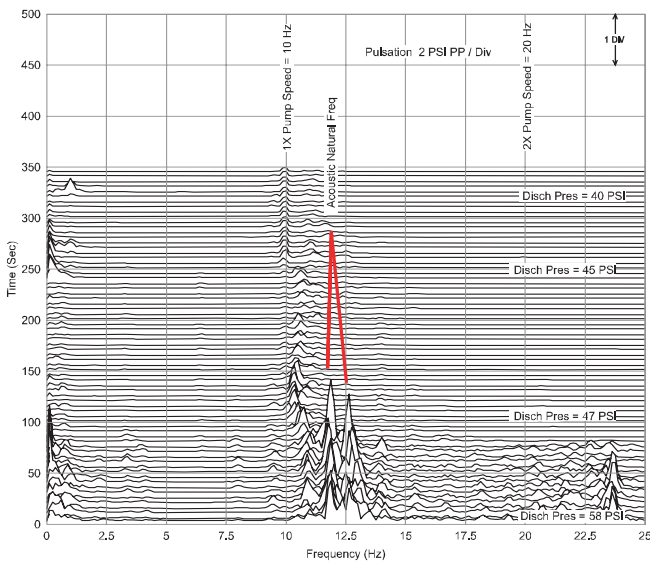


Figure 23. Pulsation at Condenser During Throttling Test of Condenser Outlet Valves as Discharge Pressure was Reduced from 3.9 to 2.6 Bar (56.5 to 37.7 PSI).

The sudden increase in broadband energy as the discharge pressure was increased and the flow was decreased is a characteristic of recirculation inside the pump. Because of the particulate matter that was suspended in the water in the sump, it was possible to visualize inlet flow characteristics using underwater video cameras. Videos near the pump inlet bell showed that the turbulence near the inlet bell was low when one pump was in service; however, when a second pump was started there was a sudden backflow when the discharge pressure was increased. This backflow was another indication of suction recirculation.

Second Field Test

The pulsation data from the first field tests indicated that the pumps were experiencing “suction recirculation.” Typically this behavior occurs at low flow conditions below the BEP on the pump head-flow curve. However, since these problems were occurring at

flow conditions to the right side of the BEP (about 110 to 120 percent), many were reluctant to agree that the pump was experiencing suction recirculation. Therefore, additional field tests were conducted. The primary objectives of these tests were:

- Determine if the sudden increase in broadband energy was due to recirculation (suction and/or discharge recirculation) inside the pump
- Determine if the sudden increase in broadband energy was due to improper flow into the pump inlet bell and/or inside the sump
- Determine if the sump generated high level discrete pulsation at the major pulsation frequencies in the band between 9 to 11 Hz
- Obtain additional pulsation data to determine the mode shapes of the major acoustic natural frequencies
- Evaluate the effects of additional underwater braces on the motor and pump column
- Evaluate the relative movement and potential mechanical contact between the impeller and the pump casing

Instrumentation

Pressure Transducers—Waterproof piezoelectric pressure transducers were installed in the sump, the pump inlet bell, the pump housing, and in the pump column (Figures 25 to 29). The pump housing was drilled and tapped for the installation of the transducers. The dynamic pressure transducers were installed in the following locations:

- **Sump**—Floor in front of the pump (east side), north wall, west wall (behind the pump), and south wall
- **Pump inlet bell**—Four locations around the circumference of the bell (45 degrees, 135 degrees, 225 degrees, and 315 degrees)
- **Pump inlet upstream of impeller**—Three locations around the circumference of the housing approximately 1 inch below the impeller (135 degrees, 225 degrees, and 315 degrees)
- **Pump discharge downstream of impeller**—Four locations around the circumference of the housing approximately 1 inch above the impeller (45 degrees, 135 degrees, 225 degrees, and 315 degrees)
- **Pump discharge column**—Midpoint of pump column between the impeller and the discharge head

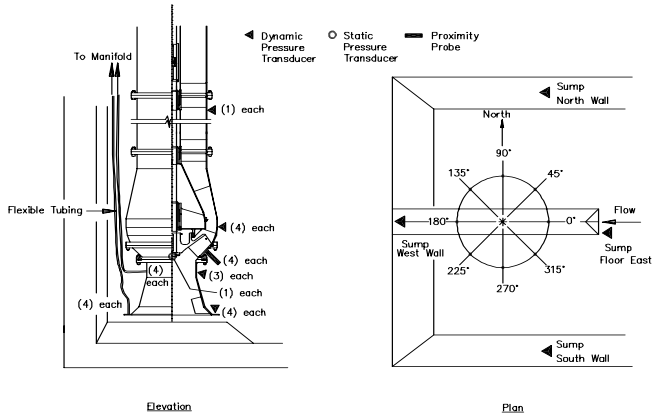


Figure 25. Sketch Showing Locations of Instrumentation on Pump Housing and in the Sump During Second Test.



Figure 26. Instrumentation on Pump Housing and in the Sump During Second Test.

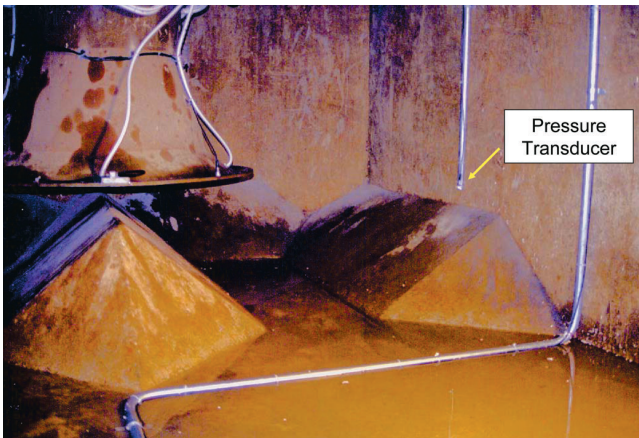


Figure 27. Instrumentation on Pump Inlet and North Sump Wall.

An additional static pressure transducer was installed in the pump inlet approximately 1 inch below the impeller at the 45 degree position (Figure 25). This transducer was not waterproof and was installed in a watertight container attached to the pump housing (Figure 26).

The pump manufacturer's representative suggested that additional static pressure data should be obtained at several locations on the pump inlet bell and near the impeller. These data would be helpful in inferring any distortion of the flow pattern at

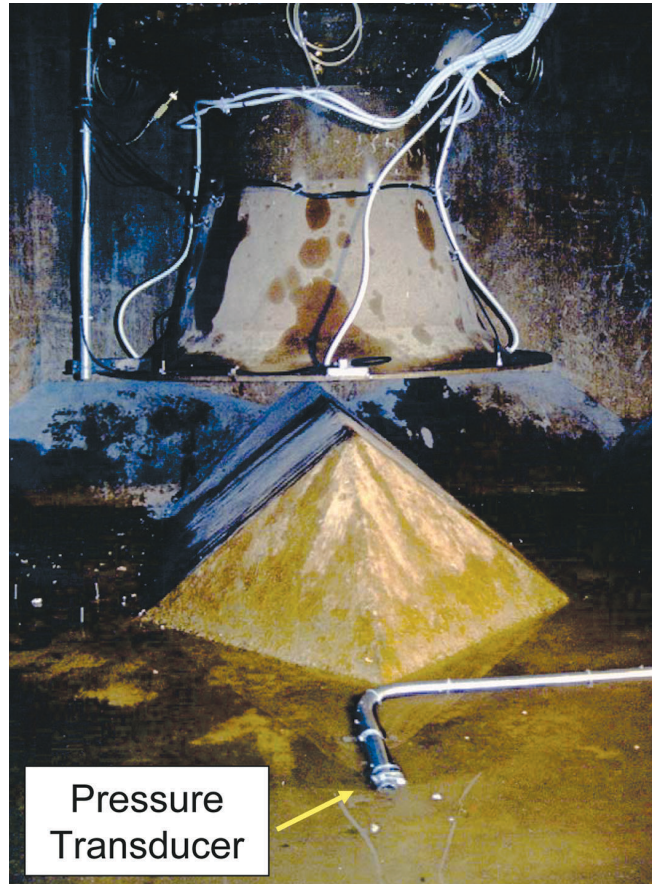


Figure 28. Instrumentation on Pump Inlet and Floor of Sump.

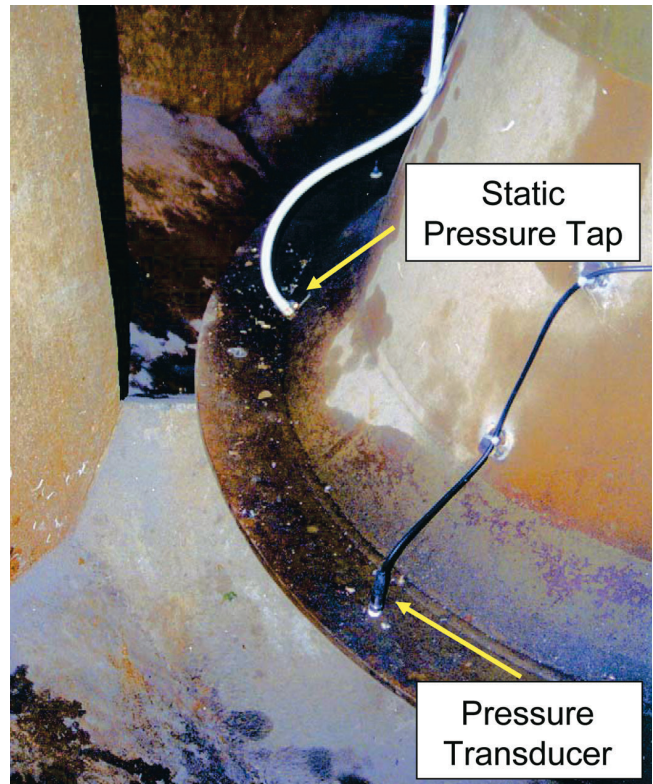


Figure 29. Static Pressure Taps and Dynamic Pressure Transducers on Pump Inlet Bell Housing.

the bell inlet and also near the impeller eye. Since additional static pressure transducers were not readily available, it was suggested that the static pressure data could be obtained by installing tubing at the desired locations and reading the static pressure at the end of the tubing at a location above the sump.

As shown in Figures 25 to 29, flexible tubing was installed at four locations on the inlet bell and at four similar locations 1 inch below the impeller. The tubing was connected to a manifold where the static pressure in each tube could be read using a static pressure transducer installed at the end of the manifold (Figure 30).

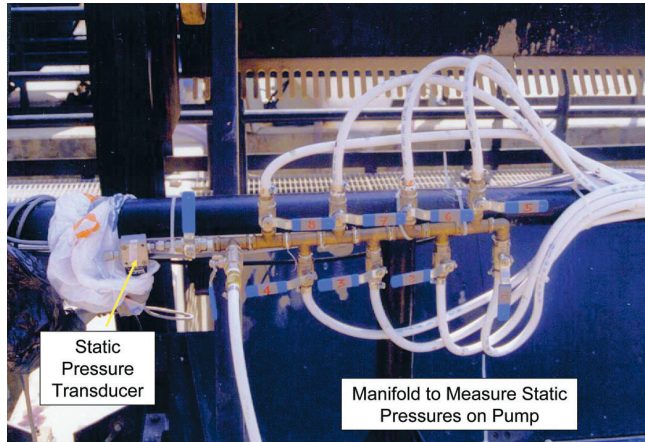


Figure 30. Manifold to Measure Static Pressures on Pump.

Prior to the tests, the manifold and each tube were filled with water and then the valves on the manifold were closed. Since the manifold was located several feet above the water surface, a negative gauge pressure was produced at the manifold due to the head of water in the tube. When the pump was in operation, the pressures in the tubes were the combined pressure due to the head of water in the tubes and the kinetic pressure at the test location. The pressures at the test locations were obtained by subtracting the head pressure.

Accelerometers—Piezoelectric accelerometers were installed on the top of the motor in the E-W and N-S directions. Waterproof triaxial piezoelectric accelerometers were installed on the pump inlet bell to measure the vibrations of the pump column.

Proximity probes—In addition to the pump shaft vibration data obtained with the proximity probes near the coupling, it was desirable to obtain shaft vibration data on the pump shaft near the impeller. However, it was determined that it would be impossible to install proximity probes without disassembling the pump. Due to time constraints, there was insufficient time to remove the pump and install the probes.

Since the probes could not be installed inside the pump, it was decided to infer the vibration of the pump shaft and impeller by installing proximity probes to measure the instantaneous relative distance between the pump shaft and the impeller vanes. The thickness of the impeller vanes was approximately 1 inch, which would provide a good “target” for the proximity probes. The probe signal was valid only when an impeller vane passed the proximity probes. Therefore, by sampling the data only when the vanes passed the probes, vibration of the impeller was determined. This sampling technique worked satisfactorily because the frequencies of interest (below 18 Hz) were below the Nyquist sampling frequency of 35 Hz (one half the impeller vane passing frequency).

Due to the test schedule, there was not sufficient time to obtain waterproof proximity probes before the tests. Therefore, normal proximity probes were waterproofed by coating the probe tip with epoxy. The probes were installed in special probe holders (Figure 31), which were threaded into the sides of the pump housing (Figure 32). The proximity probes were installed in watertight housings, which were attached to the pump housing (Figure 26).

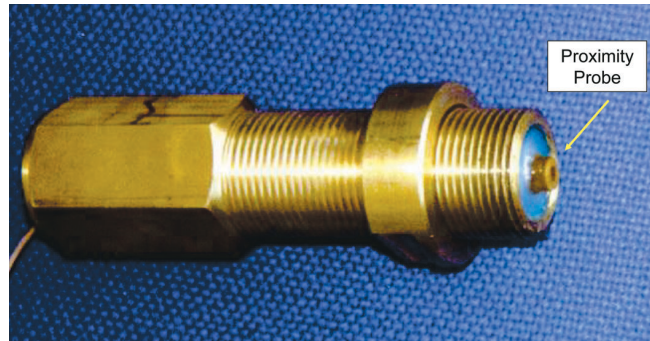


Figure 31. Proximity Probe Installed in Special Probe Holder.

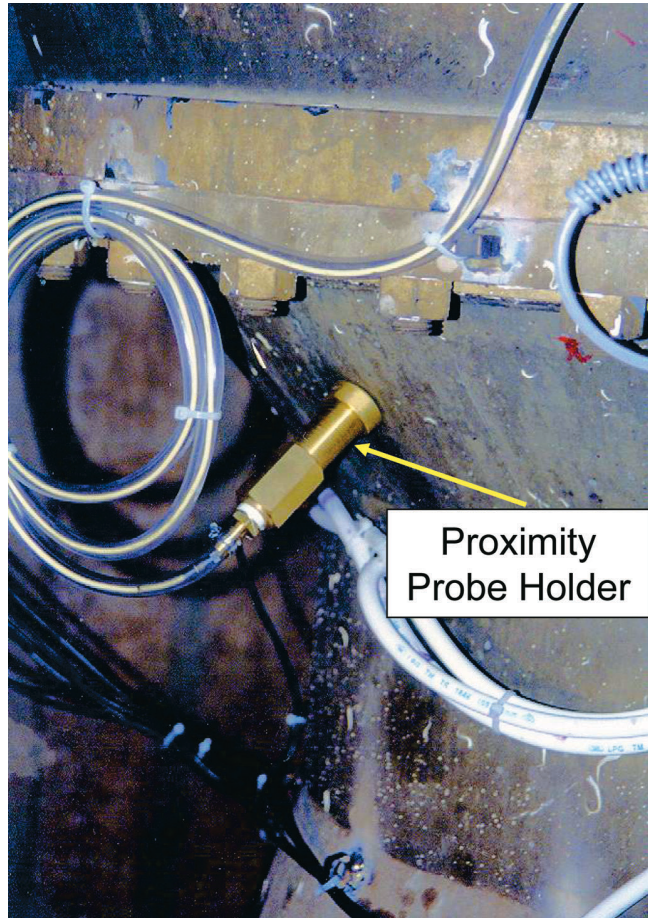


Figure 32. Proximity Probe Installed to Measure Radial Vibration of Impeller Vanes.

The probes were initially installed at four locations 90 degrees apart. The radial clearance between the impeller vanes and the wall of the pump housing was reported to be approximately 40 mils (0.04 inch). The dynamic ranges of the 5 mm (.20 inch) diameter probes were also approximately 40 mils (0.04 inch); therefore, the probes were set with a DC gap of approximately 35 mils (.035 inch) between the probes and the edge of the vanes. This caused the ends of the probes to protrude approximately 5 mils (.005 inch) beyond the edge of the housing.

During the initial startup, the probes were destroyed when they were impacted by the impeller vanes. It is thought that the impeller may have whirled-out during the startup and contacted the probes. Later inspection showed rub marks on the housing where the impeller had contacted the housing.

The 5 mm (.20 inch) diameter probes were replaced with 11 mm (.43 inch) diameter probes that had a larger dynamic range of 160 mils (.16 inch). The greater dynamic range allowed the probe tips to be recessed inside the pump wall to avoid contact with the impeller vanes.

Current probe—Motor current was measured with a current/power probe. The probe was clamped around one of the power lines to the motor. The primary purpose of the current probe was to measure current modulation of the motor during the conditions of high pulsation and high vibration.

Single Pump with Throttling at the Condenser

The suction recirculation problem was clearly identified during tests where pump A was operating alone, and one of the butterfly valves downstream of the condenser was slowly closed to raise the discharge pressure from 2.9 bar (42 psi) to 3.3 bar (47.9 psi) and consequently reduce the flow through the pump.

As shown in Figure 33, the discharge pulsation amplitudes and the suction static pressure below the pump impeller suddenly increased when the discharge pressure was increased to 3.2 bar (46.4 psi). The sudden increase in the suction static pressure is a classical indication of suction recirculation (Fraser, 1981; Schiavello and Sen, 1980). This is always characterized with backflow coming out from inside the impeller and moving into the suction pipe/suction bell. The occurrence of sudden backflow at the suction bell inlet, indicative of sudden suction recirculation at the impeller eye, was clearly observed and previously recorded with an underwater video.

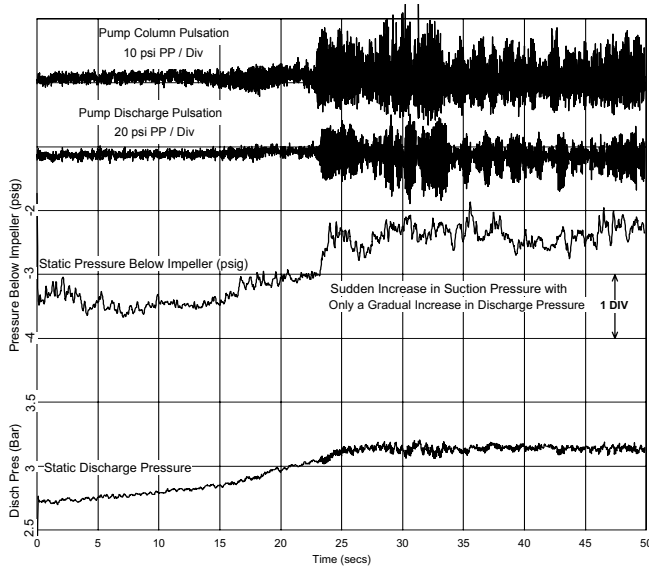


Figure 33. Pulsation and Static Pressures During Throttling Test of Condenser Outlet Valves as Discharge Pressure was Increased from 2.9 to 3.3 Bar (42.1 to 47.9 PSI).

When the discharge pressure increased to 3.2 bar (46.4 psi), the pulsation amplitudes simultaneously increased in the sump, at the pump inlet, upstream of the impeller, and downstream of impeller (Figures 34 and 35). The simultaneous sudden increase in pulsation in both the pump inlet and outlet indicated that there is one recirculation zone between the inlet and outlet connected through the impeller, rather than two separate recirculation zones (Kaupert and Staubli, 1999b).

The major pulsation response occurred at 11 Hz at all the test locations. Similar increases were measured on all the dynamic pressure transducers installed in the sump, in the pump case, and in the discharge piping. These data indicated that the suction recirculation excited the acoustic natural frequency of the pump/piping system at 11 Hz.

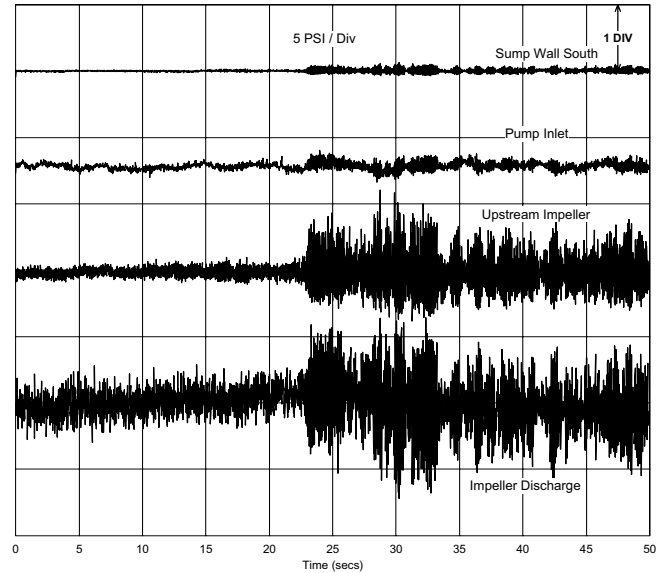


Figure 34. Pulsation at Sump Wall, Pump Inlet, Upstream of Impeller, and Downstream of Impeller at 315 Degrees During Throttling Test of Condenser Outlet Valves as Discharge Pressure was Increased from 2.9 to 3.3 Bar (42.1 to 47.9 PSI).

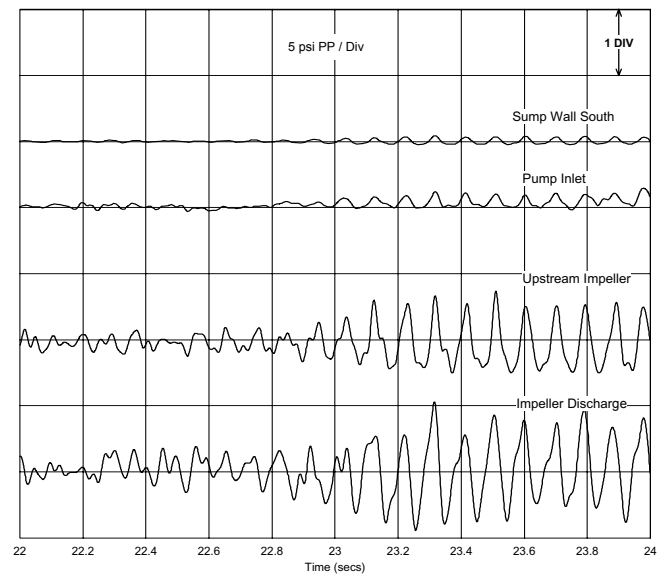


Figure 35. Zoom View of Figure 34 at Start of Recirculation Condition.

As shown in Figures 34 to 36, the sudden increase in pulsation levels occurred at approximately time = 23 seconds. The zoom plot in Figure 36 with the pulsation and the tach signal shows that the pulsation levels increased during a single shaft rotation between 23 and 23.2 seconds. These data also show that the recirculation occurred very rapidly when the discharge pressure reached the threshold pressure and also the flow reached a critical value (suction recirculation onset capacity [Schiavello, 1975; Schiavello and Sen, 1980]).

During the time before the recirculation condition, the pulsation was not phase coherent; however, the pulsation became phase coherent during the recirculation (after time = 23 seconds). Also, note that the pulsation amplitudes varied around the circumference of the housing. The pulsation data are shown in Figure 36 where the pulsation signals at similar locations were superimposed on each other for ease of comparison.

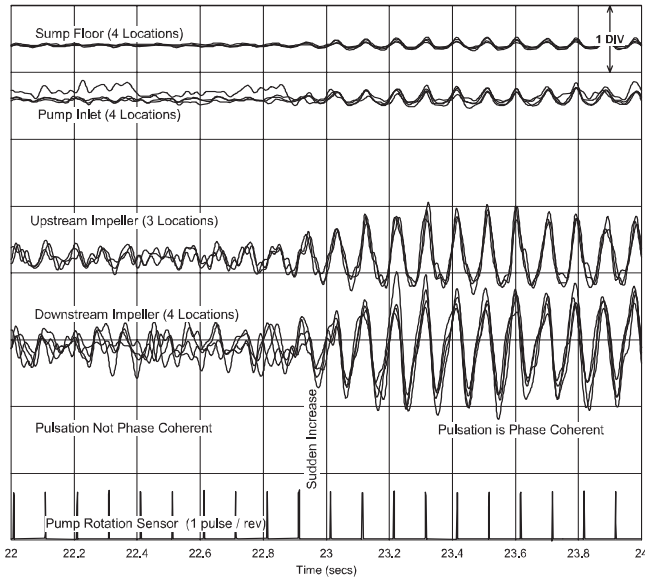


Figure 36. Zoom View of Pulsation at Sump Wall, Pump Inlet, Upstream of Impeller, and Downstream of Impeller at All Locations, and Tach Signal During Throttling Test of Condenser Outlet Valves as Discharge Pressure was Increased from 2.9 to 3.3 Bar (42.1 to 47.9 PSI).

As shown in the time domain plots and the frequency spectra, during the recirculation the pulsation occurred at a fairly pure frequency near 11 Hz (Figures 37 to 42). The frequency spectra also showed that the pulsation at the vane-passing frequency did not change during the recirculation condition.

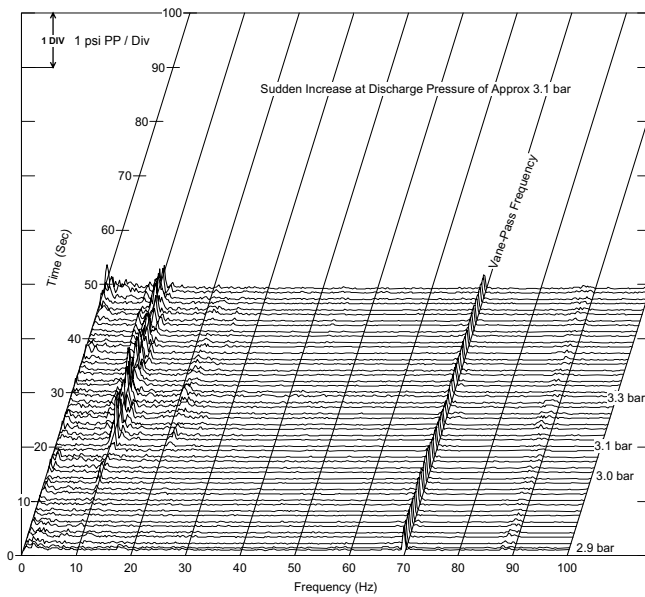


Figure 37. Frequency Spectra of Pulsation at Sump West Wall During Throttling Test of Condenser Outlet Valves as Discharge Pressure was Increased from 2.9 to 3.3 Bar (42.1 to 47.9 PSI).

Prior to the recirculation condition, the motor vibration occurred primarily at the mechanical natural frequencies of the pump column. When the recirculation began, the motor vibration significantly increased at 11 Hz because the pulsation was coincident with the mechanical natural frequency of the motor at 11 Hz (Figure 43).

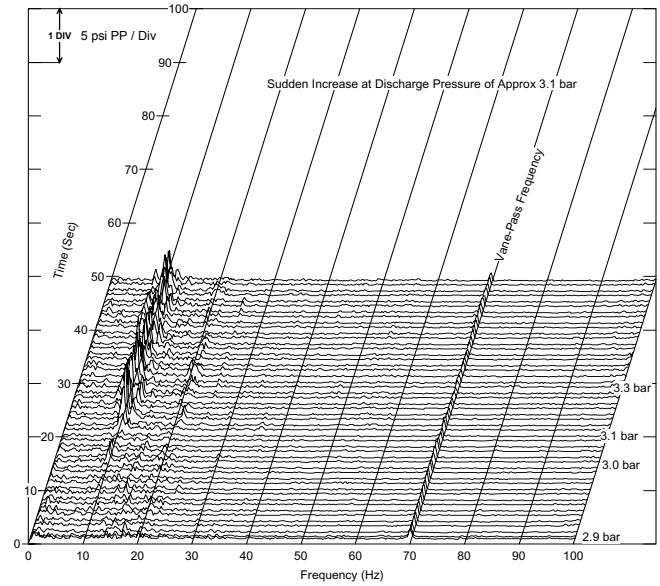


Figure 38. Frequency Spectra of Pulsation at Pump Inlet (135 Degrees) During Throttling Test of Condenser Outlet Valves as Discharge Pressure was Increased from 2.9 to 3.3 Bar (42.1 to 47.9 PSI).

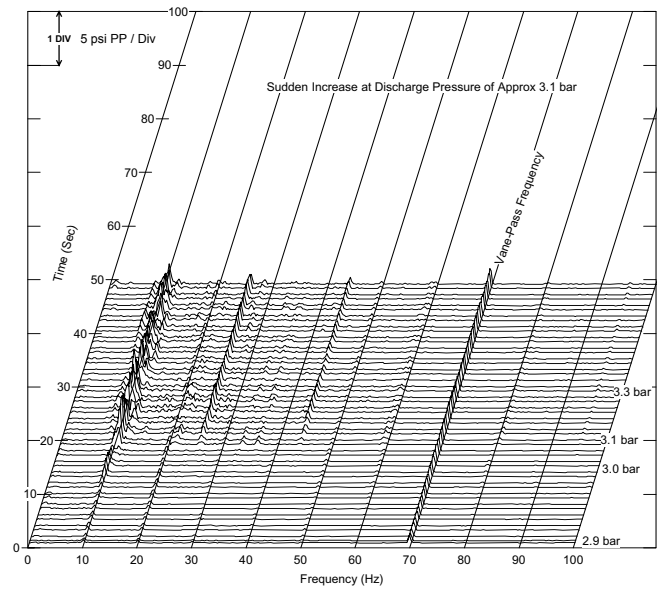


Figure 39. Frequency Spectra of Pulsation Upstream of Pump Impeller (135 Degrees) During Throttling Test of Condenser Outlet Valves as Discharge Pressure was Increased from 2.9 to 3.3 Bar (42.1 to 47.9 PSI).

The static pressure data obtained with the tubing attached to the pump housing suggested that there was a variation in the pressure data around the inlet bell that indicated that the flow velocities were different at various locations around the inlet bell. The pressures were apparently more uniform at the test locations near the pump impeller, which suggested that the inlet bell improved the flow at the entrance to the impeller. These test results generally agreed with the pulsation data obtained with the dynamic pressure transducers that showed that the pulsation levels were not constant around the circumference of the inlet bell and at the throat of the impeller. The static pressure data are described in greater detail later in this paper.

The underwater triaxial accelerometers mounted on the pump housing functioned well at low discharge pressures when the

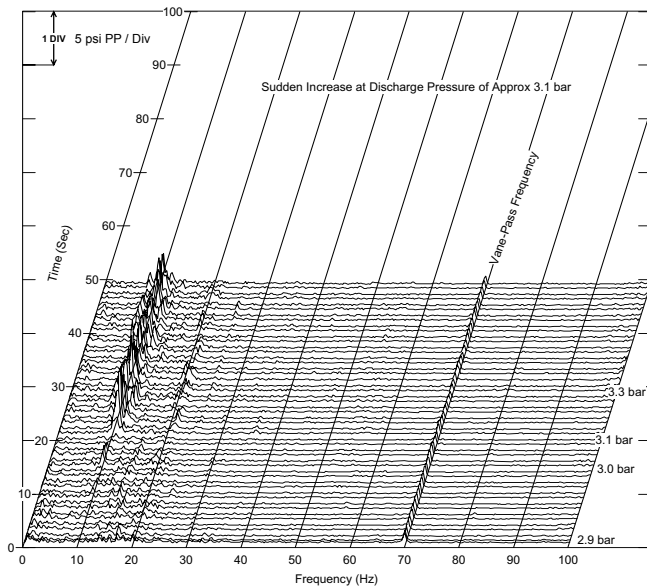


Figure 40. Frequency Spectra of Pulsation Downstream of Pump Impeller (135 Degrees) During Throttling Test of Condenser Outlet Valves as Discharge Pressure was Increased from 2.9 to 3.3 Bar (42.1 to 47.9 PSI).

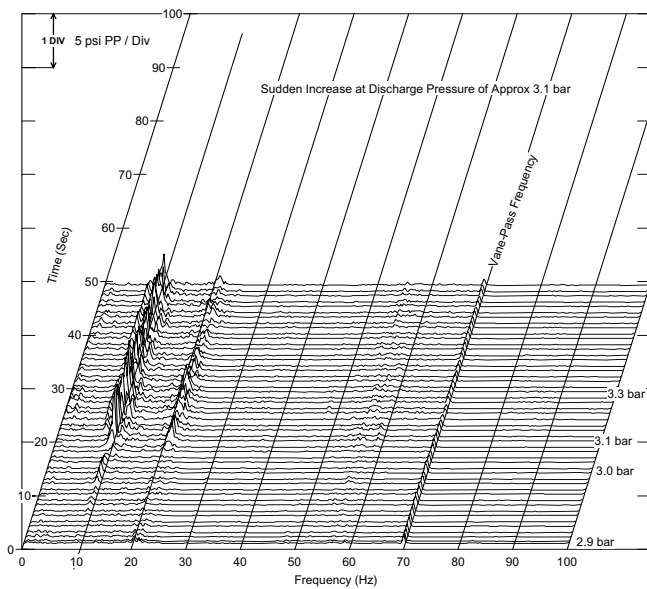


Figure 41. Frequency Spectra of Pulsation in Pump Column During Throttling Test of Condenser Outlet Valves as Discharge Pressure was Increased from 2.9 to 3.3 Bar (42.1 to 47.9 PSI).

recirculation conditions were not present. However, when the recirculation occurred, the vibration levels on the pump column were excessive, which caused the accelerometers to overload. The high acceleration levels also overloaded the amplifiers. Therefore, no vibration data were obtained on the pump column during the periods of recirculation.

Single and Two-Pump Operation at Higher Discharge Pressures

Additional tests were conducted with single and two-pump operation to determine the effects of increasing the discharge pressures above 3.2 bar (46.4 psi). These tests showed that the pulsation levels near 11 Hz increased as the discharge pressure levels increased. The tests with the higher discharge pressures had

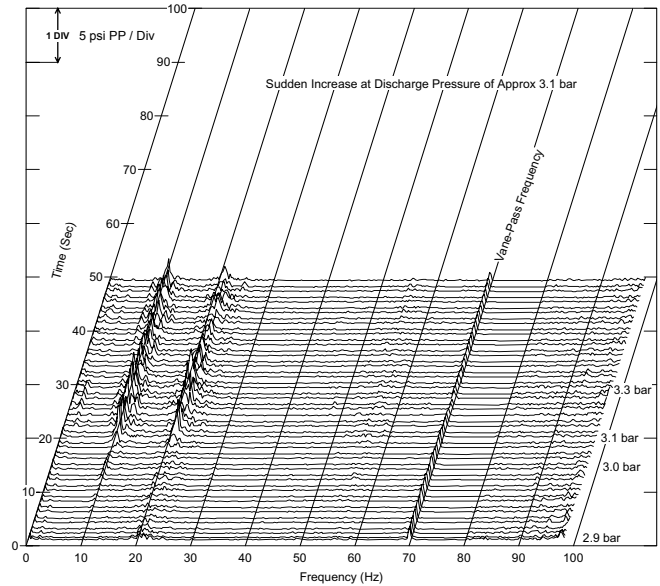


Figure 42. Frequency Spectra of Pulsation at Pump Discharge During Throttling Test of Condenser Outlet Valves as Discharge Pressure was Increased from 2.9 to 3.3 Bar (42.1 to 47.9 PSI).

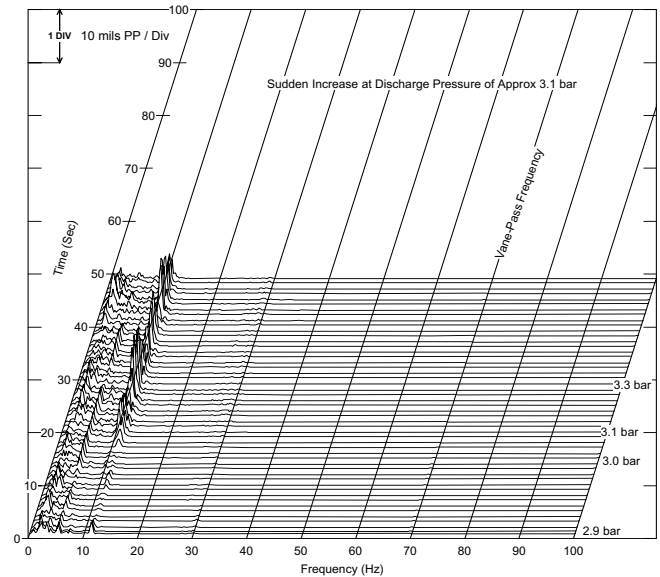


Figure 43. Frequency Spectra of Motor Vibration (N-S Direction) During Throttling Test of Condenser Outlet Valves as Discharge Pressure was Increased from 2.9 to 3.3 Bar (42.1 to 47.9 PSI).

to be terminated at 4.0 bar (58 psi) for the single-pump operation and at 3.8 bar (55.1 psi) for the two-pump operation due to excessive noise levels that appeared to emanate from the pumps.

Impeller Vibration

As shown in Figure 44, the pump impeller vibration levels were approximately 5 to 6 mils (.005 to .006 inch) peak-to-peak at the pump running speed (10 Hz) when the pump was operating at discharge pressures below 3.2 bar (46.4 psi) where the recirculation did not occur. Some of this indicated vibration could be due to mechanical runout; however, the vibration levels at this condition would be considered to be satisfactory.

When the discharge pressure was increased to 3.3 bar (47.9 psi) and the pump was in recirculation, the vibration levels on the impeller increased to approximately 15 to 20 mils (.015 to .020 inch) peak-to-peak at a frequency near 18 Hz (Figure 45). The

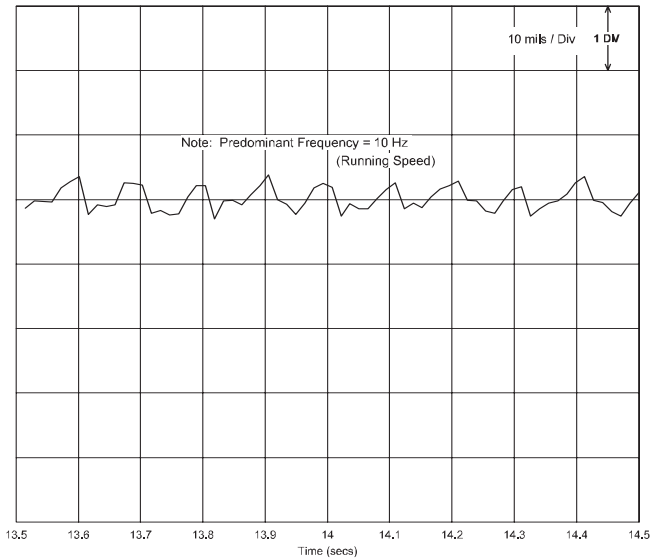


Figure 44. Pump Impeller Vane Vibration During Throttling Test of Condenser Outlet Valves as Discharge Pressure was Increased to 3.0 Bar (43.5 PSI).

impeller vibration at 18 Hz continued to increase as the discharge pressure was raised and flowrate was reduced. At a discharge pressure of 3.8 bar (55.1 psi), the impeller vibration levels increased to approximately 20 to 30 mils (.02 to .03 inch) peak-to-peak at 18 Hz (Figure 46). These impeller vibrations were considered to be excessive.

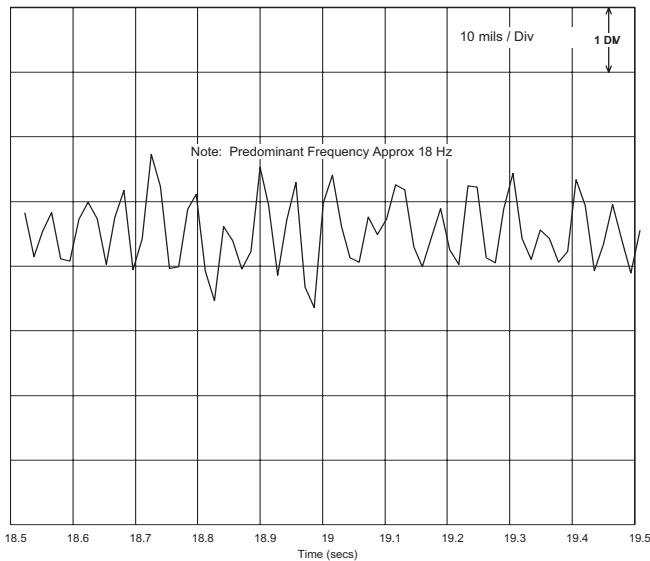


Figure 45. Pump Impeller Vane Vibration During Throttling Test of Condenser Outlet Valves as Discharge Pressure was Increased to 3.3 Bar (47.9 PSI).

The impeller vibration at 18 Hz compares to the shaft vibration measured near the coupling during the first field test. The shaft and impeller vibration data suggest that the vibration at 18 Hz was probably the pump rotor lateral natural frequency that was excited by the broadband energy produced when the pump was operating in the recirculation condition.

Analysis of the Motor Current

Frequency analyses of the motor current indicated that the amplitudes at the electrical line frequency of 50 Hz were similar to

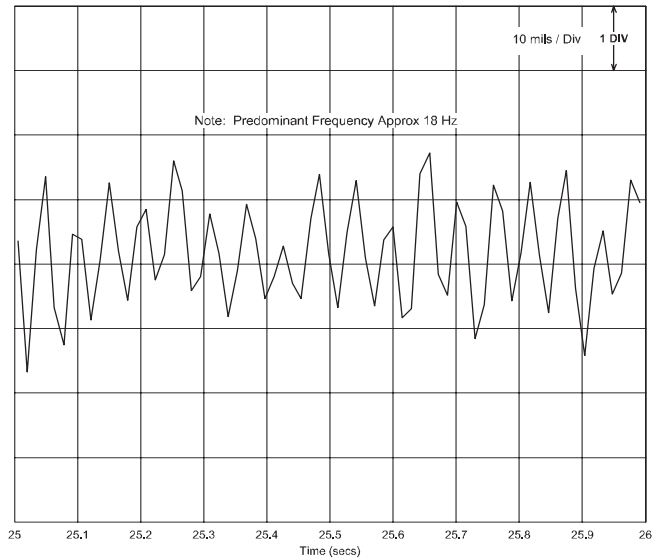


Figure 46. Pump Impeller Vane Vibration During Throttling Test of Condenser Outlet Valves as Discharge Pressure was Increased to 3.8 Bar (55.1 PSI).

the levels shown on the meter at the motor switch gear. When the pump was operating with a discharge pressure of 2.8 bar (40.6 psi), the motor current was primarily at the electrical line frequency of 50 Hz (Figures 47 and 48). During the recirculation condition at the discharge pressure of 3.5 bar (50.8 psi), sidebands were measured at approximately ± 11 to 12 Hz. The amplitudes of these sidebands were approximately 1 percent of the amplitude at the line frequency. It was felt that these sidebands were due to the fluctuation of the motor load at 11 to 12 Hz, which was caused by the high pulsation levels during the recirculation. These data suggested that the pump recirculation could also be detected by making frequency analyses of the signals from a current transformer (CT). However, further investigation would be needed.

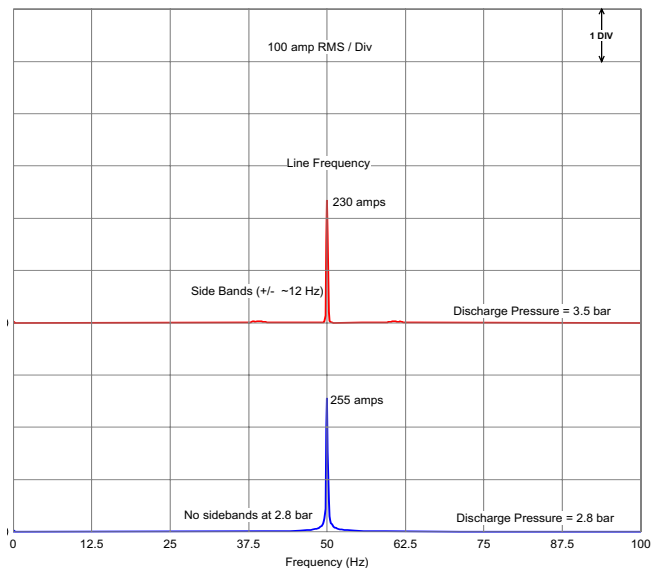


Figure 47. Frequency Spectra of Motor Current During Throttling Test of Condenser Outlet Valves as Discharge Pressure was Increased from 2.8 to 3.5 Bar (40.6 to 50.8 PSI).

Acoustic Analysis

The sudden increase in broadband energy due to recirculation excited a major acoustic natural frequency of the pump/piping

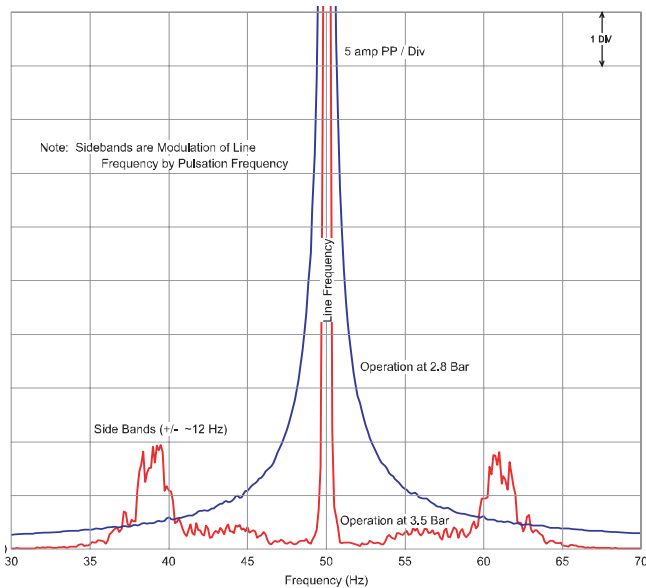


Figure 48. Zoom View of Figure 47.

system at approximately 11 Hz, which further amplified the pulsation levels. The pulsation data indicated that the mode shape for the acoustic natural frequency had minimum amplitudes at the pump inlet bell (open-end boundary condition). The pulsation amplitudes steadily increased from the inlet bell through the impeller. The maximum amplitudes occurred near the midpoint of the pump column. The pulsation amplitudes were reduced near the pump discharge flange. Although the maximum pulsation amplitudes occurred inside the pump, this acoustic natural frequency also amplified the pulsation levels throughout the piping system from the pumps to the condenser.

An acoustic analysis of the pump/piping system was made in an effort to verify the acoustic natural frequencies of the system and to evaluate possible modifications to shift the acoustic natural frequency away from the motor mechanical natural frequency near 11 Hz. The computer model included the three pumps, the piping between the pumps and the condenser, and the condenser. The model was terminated downstream of the condenser where the piping was open to the atmosphere. Geometry plots of the computer model are shown in Figure 49. Pulsation test points are noted on the geometry plots. The computer model was excited at one of the pump impellers using a uniform pressure excitation at all frequencies between 1 to 25 Hz.

The computed acoustic natural frequency and mode shape near 11 Hz agreed well with the measured field data. The computed normalized pulsations at the pump discharge flange and at the condenser are shown in Figures 50 and 51. The computer analyses indicated that the predominant acoustic natural frequency near 11 Hz was primarily associated with the pumps and the pump manifold piping.

The frequency of this mode was sensitive to the compliance of the expansion joint at the pump discharge flange. During the field tests, dial indicators were used to measure the radial expansion of the joint over the range of discharge pressures. These data were used to compute the compliance values of the expansion joint that were input into the computer model. The effect of the flexibility of the expansion joints was similar to that of an inline gas charged accumulator.

The analyses indicated that the acoustic natural frequency of the system could be raised from 11 Hz to approximately 19 Hz by replacing the expansion joint at the pump discharge flange with a rigid section of piping. The acoustic natural frequency near 19 Hz would still be excited by the recirculation, but the pulsation at the acoustic natural frequency would no longer be coincident with the major mechanical natural frequency of the motor near 11 Hz. This

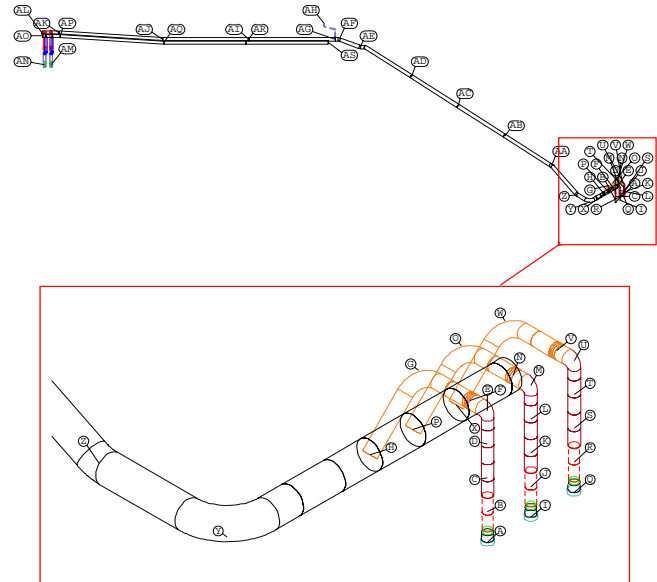


Figure 49. Geometry Plot of Acoustic Model of Cooling Water Pump System.

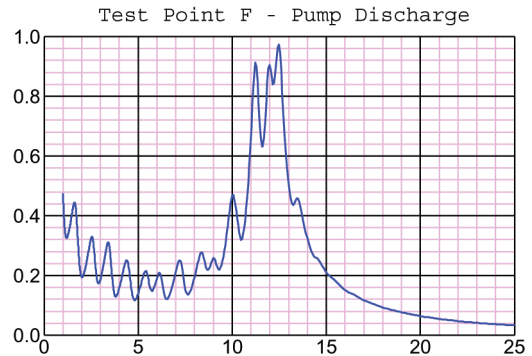


Figure 50. Computed Pulsation at Pump Discharge with Excitation at Impeller of Pump A.

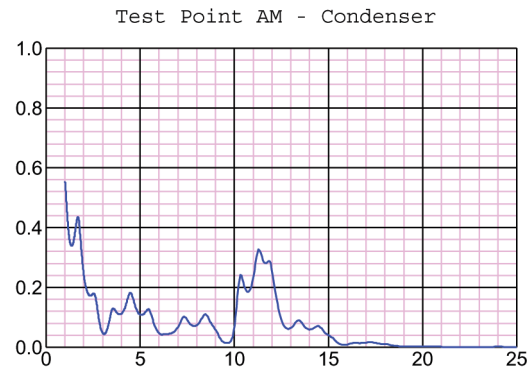


Figure 51. Computed Pulsation at Condenser with Excitation at Impeller of Pump A.

potential modification was not recommended, however, since shifting the acoustic natural frequency to 19 Hz could possibly increase the pump rotor vibration at the pump rotor lateral frequency near 18 Hz.

SOLUTION STRATEGY— APPROACH AND FIELD IMPLEMENTATIONS

The data measured during the second field tests confirmed that the pumps were experiencing recirculation during two-pump

operation and during single-pump operation when the discharge pressure was increased above 3.2 bar (46.4 psi). The suction recirculation condition produced broadband turbulence (pulsation), which excited the acoustic natural frequency of the pump/piping system near 11 Hz, and several mechanical natural frequencies of the motor/pump between 3 to 11 Hz. The coincidence of the acoustic natural frequency and mechanical natural frequency of the motor near 11 Hz resulted in the excessive vibration levels on the motor.

Moreover, the field data indicated that the recirculation condition was occurring at a pump head of approximately 40 m (131 ft) and a flowrate of 14,500 m³/hr (63,842 gpm). This operating condition was above the rated point and 120 percent of BEP capacity. As discussed, the occurrence of the recirculation at flowrates well above the BEP is an abnormal situation beyond the current knowledge of both the manufacturer's experience and the open technical literature.

The solution strategy was discussed and agreed upon among the end user, the contractor, the engineering company, and the pump manufacturer. The main focus was on the fluid interaction between the suction system and the pump, which can be identified as "suction interaction." The "discharge interaction" (discharge pressure pulsations, mechanical and acoustic interaction, motor/pump vibration) was considered as an "effect" and was left out of the first phase of the solution strategy (but still taken in mind), by realizing the complexity for field implementation of possible related modifications for the pump and system.

The approach was to:

- Correlate the field data and observations with the background data and the design of both the pump and the sumps
- Identify necessary changes for the pump and/or sumps

Fluid Review of Background Data—Pump Design

The hydraulic design of the subject pumps was fully scaled from a model, which had been previously used by the manufacturer for designing several other pumps, some of which were actually larger than the model. These other pumps were used for various services at operating conditions both above and below their BEP capacity.

The manufacturer searched its internal records looking for any warranty claim of field vibrations caused by suction recirculation, and no indications of field suction recirculation were found. Moreover, three installations were found that had pumps that were fully identical to the subject pumps (i.e., same hydraulic design, size, and operating speed) and were installed in circulation water cooling systems. It was reported that these three pump field installations operated satisfactorily over a wide range of capacities free from vibration induced suction recirculation.

The shop tests of the subject pump at full speed were reviewed looking for signs of suction recirculation and excessive vibration. A close inspection of the shop hydraulic performance (Figure 3) clearly shows a net change in the curve shape for both the head (Figure 3a) and power (Figure 3c) near 40 percent of BEP capacity and also near 40 percent of the rated capacity (as $Q_{BEP}/Q_{rated} = 1.01$), where head and power start to rise. These changes in the curves are produced by suction recirculation, as supported by literature.

A comparison can be made with a set of performance curves from another pump, where the head rise begins near 50 percent (Schiavello, 1982). Data obtained on the other pump clearly shows that the onset of suction recirculation (characterized by unsteady flow) is actually at higher capacity around 70 percent BEP. In certain cases, even a hysteresis loop between these two peculiar capacities can be observed (Kaupter and Staubli, 1999a, 1999b).

Since the detailed hydraulic design features were known by the pump manufacturer for the other pump and the subject pumps, an indirect comparison was reasonable. Therefore, it could be expected that the onset of suction recirculation for the subject

pumps would be near 60 percent of BEP (50 percent higher than the head discontinuity point at 40 percent BEP), which is well below the onset recirculation capacity in the plant at 120 percent BEP.

Shop Tests

The shop tests were performed at full speed using a test stand for vertical turbine pumps, which includes a relatively large pit having internal dimensions and characteristics that conform to the guidelines of both the pump manufacturer and the Hydraulic Institute. During the design of the pit, special attention was given with regard to providing a good approach flow at the pit inlet and a uniform steady flow pattern, free from swirl, at the suction bell inlet.

A review of the shop test vibration data measured at the top of the job motor showed perpendicular (out-of-plane) vibration of 2.9 mils (.0029 inch) peak-to-peak and parallel (inplane) vibration of 3.2 mils (.0032 inch) peak-to-peak at the rated flow capacity. The shop vibration levels remained low in the flow range of 60 to 120 percent rated capacity. These vibration levels were well below the field vibration levels at rated flow or above, which suggests the absence of hydraulic excitation, such as suction recirculation, during the shop test. Additionally, the shop test records do not mention vibration problems, even at flowrates below 60 percent BEP, where suction recirculation was likely present.

The fact that the vibration levels were acceptable during the shop tests suggested that the excessive vibration problems in the field could possibly be related to differences between the installation at the factory and at the site, which could have changed the mechanical and acoustical natural frequencies of the systems. The major differences in the shop configuration were the more flexible foundations, short discharge piping, and no expansion joint. During the shop tests, no vibration spectra were taken, which would give more clues as to the predominant vibration frequencies and amplitudes.

Incidence Angle

A hydraulic design review was performed with the focus on the incidence angle of the relative flow at the impeller inlet blade tip section, because this angle is known to have a critical role in the onset of rotating stall and suction recirculation (Schiavello and Sen, 1980). The essential physical aspect is that these phenomena occur when the incidence angle at the tip is positive and reaches high values causing a "stall" on the blade (flow separation). The incidence angle is defined as the difference between the blade (metal) angle at the leading edge and the flow angle of the relative velocity direction just before the blade leading edge.

For fixed rotational speed, the incidence angle varies only with capacity. There is one capacity at which the incidence angle is zero and is called the "shockless capacity." This capacity is usually close to the BEP capacity at the impeller outlet maximum diameter (design capacity). The incidence angle is positive below the shockless capacity and is negative above it. Clearly, the rotating stall/suction recirculation onset capacity is always below the shockless capacity for uniform inlet steady flow, especially with expected swirl velocity component included in the design calculations.

In the case of a vertical pump impeller with a suction bell, the design assumption for incidence calculation is that swirl is absent. The incidence analysis for the subject pump showed that the incidence angle at the rated flow was +1.6 degrees, $Q_{SL}/Q_R = 108$ percent (SL=shockless, R = rated), or $Q_{SL}/Q_{BEP} = 107$ percent. (Note: the job impeller was trimmed. For untrimmed impellers, the internal tests show $Q_{BEP-Max}/Q_R = 106$ percent giving $Q_{SL}/Q_{BEP-Max} = 101$ percent).

The incidence angle at the field onset recirculation capacity (14,500 m³/hr [63,842 gpm]) is 2.6 degrees. This negative value absolutely excluded the onset of suction recirculation at such

capacity as related to the impeller design. It also confirmed that an abnormal suction recirculation situation was occurring in the field and strongly suggested the presence of highly uneven (and unexpected) flow distribution at the impeller inlet induced by the suction system (intake plus sump).

Predicting Suction Recirculation

The application of empirical correlations for predicting the suction recirculation capacity from the impeller geometry (Fraser, 1981) has been considered to be invalid for vertical pumps with diagonal impellers. On the other hand, global trends linking suction recirculation effects with suction specific speed (Hallam, 1982) are essentially “gross” and not proven for vertical turbine pumps. The suction specific speed of the job pump is 10,600 (at rated capacity with trimmed impeller), while it is 10,400 at the impeller inlet design capacity, $Q_{BEP-Max}$. This value is not critical (as the $Q_{BEP-Max}$ is coinciding with the shockless capacity) enough to cause the onset of suction recirculation above BEP capacity.

Schiavello (1982) presented a comparison of various possible approaches for predicting the suction recirculation capacity of a group of experimental impellers (centrifugal-flow with radial outlet impellers). Two of these methods were applied to the subject pump in an effort to obtain a “feeling” about the susceptibility of the design to cause recirculation at high flow capacities.

The first method is called stalling incidence criterion. This method indicated quite a wide range for the stalling incidence (+3.2 to +9.0 degrees). It predicted suction recirculation onset from 65 to 80 percent BEP, which was well below the onset measured during the field tests.

The second applied method is related to the diffusion ratio (DR) ($DR = W_2/W_1$, where W = impeller relative velocity, 1-inlet, 2-outlet). The DR had a range of critical values from 0.55 to 0.85, but more likely 0.65 to 0.75. This method predicted suction recirculation from 65 to 85 percent of BEP. Again, these values were well below the flowrates where the recirculation occurred in the field tests.

Therefore, the common indication was that the suction recirculation should be expected at flowrates well below BEP, which was in agreement with the shop test curve shape. The analysis of the diffusion ratio suggested that the diffusion was stronger toward the impeller exit with the possibility of discharge recirculation. This would produce a rise of pressure pulsation and vibration at the vane passage frequency of 70 Hz (Barrand, et al., 1984). However, the field vibration spectra indicated that the pulsation at the vane passing frequency did not increase during the recirculation condition.

Static Pressure Data in the Pump Suction Bell

The wall static pressures were measured at two axial stations along the suction bell near the bell inlet “lip” just inside the first conical section and before the bell vanes, and at the bell throat near the position of the impeller eye (impeller inlet) (Figure 25). In each section, four taps were used corresponding to an angular location identified as: E = east, N = north, W = west, and S = south. The E-W direction coincided with the longitudinal symmetrical axis of the sump (E is the first point seen by the approaching flow and W is close to the sump back wall). During the field tests, static pressures were measured for a range of flows and pump discharge pressures and are given as values relative to atmospheric pressure (psig) in Tables 3 and 4. The variations of local pressure from the average values are referred to as the circumferential distortion (Tables 5 and 6).

Table 3. Data Acquired During Throttling Tests at Inlet Bell.

Discharge Pressure, Barg	Local Static Pressure, psig				
	East	North	West	South	Average
2.8	3.582	7.682	4.732	3.982	4.994
2.9	5.832	9.932	8.082	6.932	7.694
3.0	5.782	9.132	7.732	6.632	7.319
3.2	4.682	7.982	5.232	4.582	5.619

Table 4. Data Acquired During Throttling Tests at Impeller Inlet.

Discharge Pressure, Barg	Local Static Pressure, psig				
	East	North	West	South	Average
2.8	0.555	0.405	0.305	0.355	0.405
2.9	3.705	2.855	2.305	2.255	2.780
3.0	3.455	2.805	2.255	2.305	2.705
3.2	1.555	0.955	0.955	0.955	1.105

Table 5. “Circumferential Distortion” at Inlet Bell.

Discharge Pressure, Barg	Local Static Pressure Variation from Average, psia			
	East	North	West	South
2.8	-1.413	2.688	-0.263	-1.013
2.9	-1.863	2.238	0.388	-0.762
3.0	-1.538	1.813	0.413	-0.688
3.2	-0.938	2.363	-0.388	-1.038

Table 6. “Circumferential Distortion” at Impeller Inlet.

Discharge Pressure, Barg	Local Static Pressure Variation from Average, psia			
	East	North	West	South
2.8	0.150	0.000	-0.100	-0.050
2.9	0.925	0.075	-0.475	-0.525
3.0	0.750	0.100	-0.450	-0.400
3.2	0.450	-0.150	-0.150	-0.150

These variations from the average pressure are plotted in Figure 52 for the suction bell inlet and Figure 53 for the impeller inlet in correspondence to the field test points unaffected by suction recirculation ($P_{disch} = 2.8, 2.9, \text{ and } 3.0 \text{ barg}$ [40.6, 42.1, and 43.5 psig]) and at the onset of suction recirculation ($P_{disch} = 3.2 \text{ barg}$ [46.4 psig]).

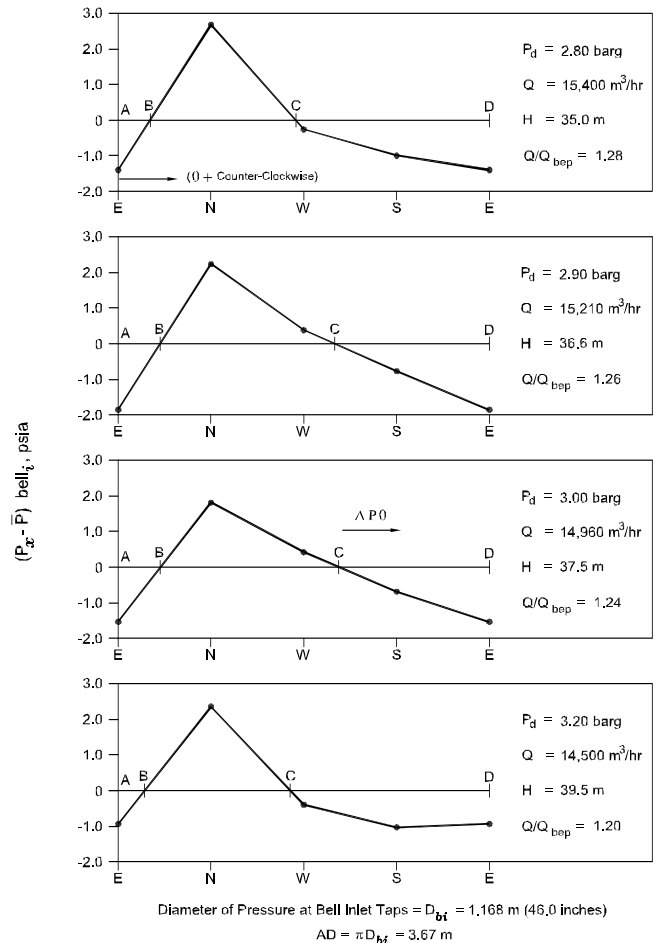


Figure 52. Local Static Pressure Variation at Suction Bell Lip (PSIA).

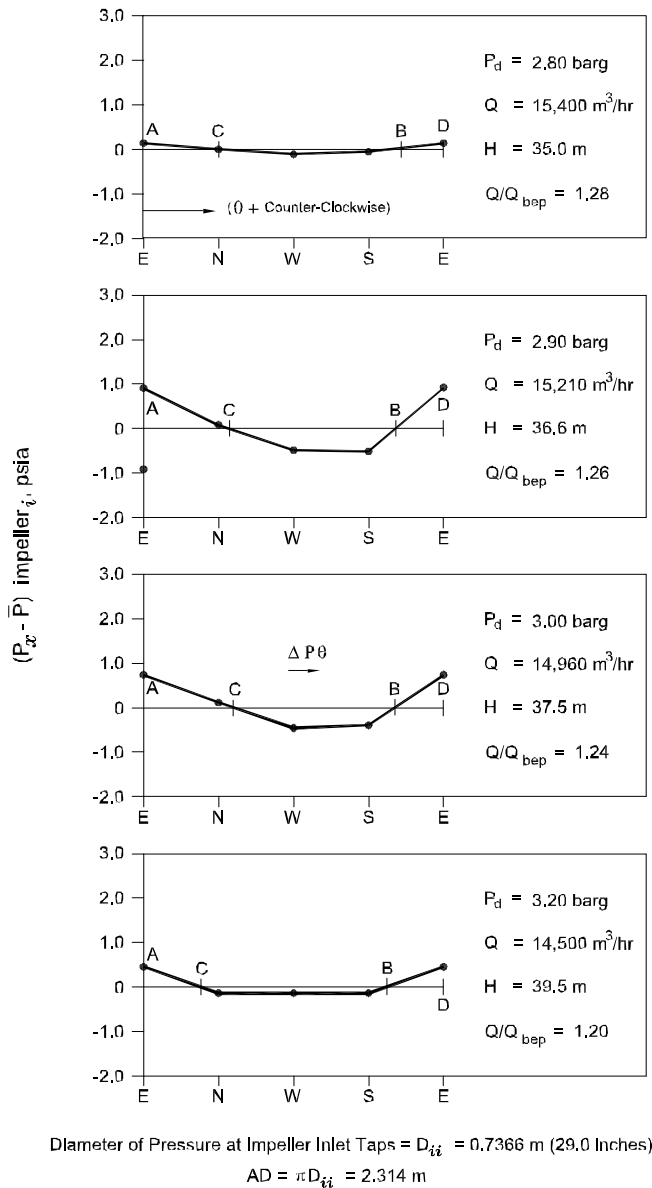


Figure 53. Local Static Pressure Variation at Impeller Inlet (PSIA).

If it is assumed that the total pressure is more or less equal for all streamlines crossing the section (i.e., an equal pressure loss from upstream conditions), then a negative deviation of static pressure corresponds to:

- A positive variation of the local axial velocity component above the average, which would result in higher local mass flow (local flow surplus), positive flow unbalance, and/or
- A presence of a tangential velocity component (swirl component).

On the other hand, a positive deviation of static pressure corresponds to a local reduction of the axial velocity (i.e., local deficit of mass flow) even down to zero (pressure deviations exceed the average velocity head calculated by assuming in the first iteration that the total flow area is equal to the full geometrical area).

Looking at the static pressure measurements at the bell inlet (Figure 52), the following observations can be made:

- A negative variation occurred at the E-point (i.e., high local velocity) where the longitudinal wedge baffle reduces the clearance under the bell.

- A positive variation occurred at the N-point. The pressure variation is higher than the average velocity head for all flows shown indicating a zone with zero through-flow. The angular extension with positive deviation (zero or flow deficit) extends for about 40 percent of the angular periphery (ratio BC/AD).

- A decrease of static pressure occurred from N to E via W-S, which suggests the presence of a distorted tangential velocity (swirl component).

- A rapid increase of pressure occurred between the E-point and the N-point, which suggests a rapid change of local tangential velocity (i.e., a shear flow).

- A radial pressure and velocity gradient may exist also.

This highly distorted flow pattern at the bell inlet was very likely produced by the intake sump configuration.

Looking at the impeller inlet static pressure data (Figure 53), the static pressure distortion is nearly eliminated at the highest flow ($P_d = 2.8$ barg [40.6 psig]) which is likely an effect of the acceleration of the axial velocity along the suction bell and also a deswirling action of the three ribs at the bell inlet. However, the static pressure distortion is evident at flows before the onset of suction recirculation ($P_{disch} = 3.0$ barg [43.5 psig]).

The negative and positive deviations at the impeller inlet are both attenuated, thus suggesting a more equalized axial velocity and mass distribution. The highest flow deficit at the E-point is approximately 6.0 percent. The angular pressure gradient is still present with a value comparable to the one at the bell inlet (at $P_{disch} = 3.0$ barg [43.5 psig], the gradient is 1.04 psia/m at the impeller inlet versus 1.36 psia/m at the bell inlet for the N-S direction). Therefore, the presence of swirling flow at the impeller inlet can still be suspected along with a radial gradient of both pressure and velocity, which makes the flow pattern in front of the impeller different from the design assumptions (namely for assessing the incidence angle, the impeller vane loading, and the diffusion ratio).

Fluid Review of Background Data—

Suction System Design (Intake-Sump)

The site suction system (suction piping and three sumps) is shown in Figures 8 and 9. The visual observations of the water in the sumps are summarized as follows:

- *Pump A operating alone*—A wave motion of the water surface was present that passed from the front wall at the suction exit flange to the curtain wall (“skimming wall” shown in Figure 9) through the trash rack toward the pump and then returned back from the pump.
- *Pump A and B operating in parallel*—Intermittent surface vortices were formed near the curtain wall (on the pump side). The sump B was more turbulent than sump A.
- *Pump B and C operating in parallel*—Sump C was more turbulent than sump B. Also, the water surface was very turbulent (sump C) between the inflow pipe and the curtain wall. The turbulence persisted between the curtain wall and the trash rack.

During the process of instrumenting the suction bell, the authors spent a considerable amount of time near the bell inside sump A. Looking from the bell location toward the exit flange of the suction piping, it was observed that the flange area was fully visible below the bottom edge of the curtain wall.

It was hypothesized that the jet flow stream coming out of the inlet flange would find small resistance and minor energy dissipation from the curtain wall and from the trash rack due to the large grid (Rosenberger, 1997). The jet flow stream would reach the suction bell with an uneven fluctuating velocity profile instead of spreading across the full width of the sump. The visual observations of the flow turbulence in the space between the exit flange and the

curtain wall, and also behind the curtain wall, suggested that the flow turbulence could be linked to the persistence of the jet stream.

Comparisons Between the Scaled Model and the As-Built Sump

Prior to construction, a model study of the suction system was performed by an independent laboratory for the engineering and construction company. (Note that the data from the hydraulic model studies shown in this paper were compiled from the model study reports.) After the above field observations, a close review of the model test report was made by the pump manufacturer. The first step was to make a detailed comparison of the key geometrical dimensions and sump internal features (wedge baffle, corner fillers, etc.) between the as-built sump (construction drawings and actual site measurements) and the test model.

Four deviations were found—three were considered to be minor with negligible influence on the flow pattern at the suction bell inlet, and one crucial (i.e., the open clearance between the bottom edge of the curtain wall and the sump floor was higher in the site compared to the final model recommendations). Namely, in the final model layout, the curtain wall was extended further down and was partially blocking the jet exiting from the intake piping.

As shown in Figure 54, the model was built using a geometry scale of 1:7 and included all three circulating-water pump bays, the auxiliary water pump located in one bay, and major structural features likely to affect flow through the pump structure. Also, the model layout included part of the suction piping leading to the bays, specifically, the main collector and the three lateral T-branches connecting each sump.

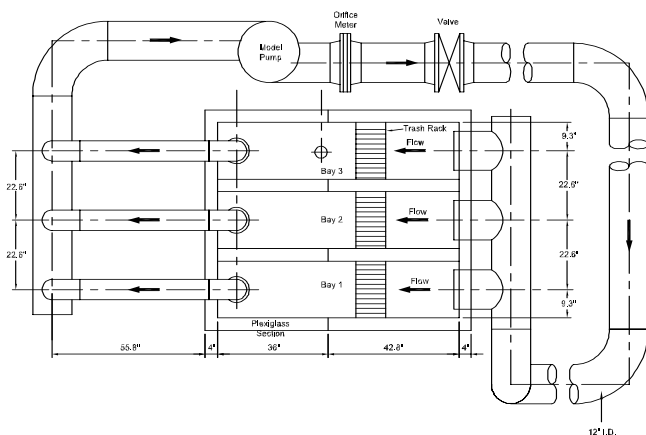


Figure 54. Scaled Model of Circulating-Water Pump Structure, Plan View.

The modeling was conducted in conformity with the Froude number scaling criterion, which is the usual approach for modeling flow processes involving a free surface, making allowance for the effects of water viscosity, and surface tension on flow patterns (governed by Weber number). The Froude number is defined as:

$$F = \frac{V}{\sqrt{gL}} \quad (3)$$

where:

V = Flow velocity (usually average velocity across the sump width)
L = Characteristic length (e.g., the water depth)

The Froude number similarity means: $F_m = F_p$ (subscripts m and p refer to model and prototype, respectively). With a geometrical scale factor of 7:1 (prototype to model), the velocity factor was 2.64 and the capacity factor was 129.6.

Simulation of viscous forces (energy dissipation) requires that: $Re_m = Re_p$ (Reynolds number similitude). This is not usually feasible, but it is considered that the model provides accurate results if Re_m (based on the sump cross-flow velocity and depth) is

above 600, which is the critical value required to yield turbulent flow conditions in the model as for the prototype. It should be noted that this Reynolds number refers to the cross-flow in the sump, not to the flow in the T-branches or to the jet stream entering the sump.

The suction bell was accurately scaled down (Figure 55) and was included in the model tests. The through-flow velocity distribution was measured at the "throat" of the bell (corresponding to a plane near the impeller eye). Also, the rotational speeds of pump-approach flows were measured by using a vortimeter (a four-bladed, zero-pitch propeller mounted on low friction bearings). Visualizations of the flow pattern across the sump were made and measurements of the velocity profile were performed.

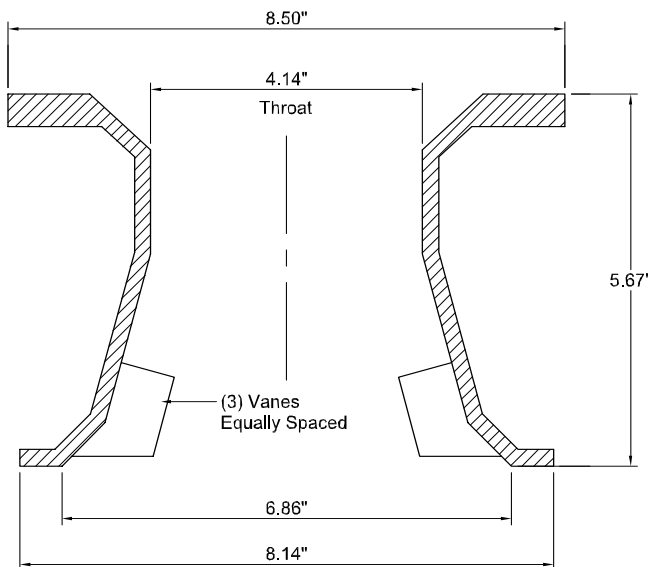


Figure 55. Sketch of Modeled Pump Suction Inlet Bell.

In essence, the test procedures confirmed with the standard practice and accuracy for model tests. The acceptance criteria were based on the experience of the company performing the modeling tests, and on the criteria of the engineering and construction company. These criteria were in close adherence with the latest HI guidelines (ANSI/HI 9.8, 1998).

A first indicative result was observed with the first trial sump configuration (Figure 56), which produced a velocity pattern of the sump cross-flow suggesting a large swirling flow around the bell with counterclockwise rotation. This undesired aspect was basically corrected by adding the curtain wall between the inflow flange (front wall) and the trash rack and also a longitudinal (east-west) wedge baffle under the bell. The final recommended layout of the sump is shown in Figure 57, which includes a bottom clearance below the curtain wall of 1.51 m (4.95 ft) at full scale and other features to prevent vortices (various corner fillers). The model tests indicated that this design provided an acceptable sump cross-flow velocity profile (Figure 58), and a satisfactory velocity pattern at the bell throat with acceptable axial velocity distribution (maximum deviation from average below 10 percent) and practically no swirl, as shown in Figure 59.

The actual clearance below the curtain wall at the site was 1.80 m (5.9 ft) which was close to the top point of the flange allowing the jet stream to pass through, rather than the recommended height of 1.51 m (4.95 ft), which partially obstructed the inlet flange. This deviation was thought to be associated with the occurrence of distorted rotating flow near the pump, as suggested by Figure 56 (no curtain wall and no baffle). Such a flow pattern could explain the presence of distorted swirling flow at the suction bell lip, as indicated by the angular distortion of the static pressure (Figure 52) and could be a factor contributing to the abnormal suction recirculation situation.

vortices. These observations of the model did not agree with the flow observations on site, which revealed the formation of surface vortices near the sump inlet and also strong turbulence above the sump entrance section at the elbow discharge.

Additional Modifications to Sump Model

Next, several geometrical changes to the sump, which could be implemented in the field, were investigated in model test, mainly aimed at “conditioning” the flow stream under the curtain wall. The primary direction for all trials was to dampen the energy and control the direction of the turbulent separated jet outgoing from each elbow and expanding in the sump, which was recognized as the main source of the unsteady distorted flow in the sump and at the suction bell throat. Very effective changes suggested by past experience with similar suction systems (suction piping plus individual sumps) would have required the use of vanes in each T-branch and/or a full height wall (concrete or metal) with holes instead of the curtain walls. However, such drastic sump modifications were excluded for various practical reasons.

A final configuration “as-modified sump” (three posts, 1.8 m (5.9 ft) curtain wall clearance, and a floor beam) was selected that produced an acceptable steady flow distribution inside the sump and also at the bell throat (impeller eye in the field pump configuration). The model tests with these modifications revealed the following:

- Small rotation of the vortimeter with 1 to 3 rpm in the counterclockwise direction (i.e., positive prerotation relative to the impeller as recommended by the pump designer)
- Steady uniform profile across the bell throat for the axial velocity (through-flow component)
- Steady uniform velocity profile across the bay
- Steady velocity profiles of the mainstream in the sump at various flowrates

However, several potential problems with the model remained unresolved:

- The intake suction pipe flow was not fully simulated. There was a large deviation from the Reynolds number similarity of the internal flows, particularly inside the elbow, and which affected the inlet flow conditions into the sump. The Reynolds number similarity ratio was too high (i.e., $Re_p/Re_m = 7^{1.5} = 18.5$), which indicates that the inertia forces determining the jet profile in the elbow in the model test conditions are only 5 percent of the corresponding inertia forces at the site conditions, or inversely, the fluid viscous forces determining the dissipation of the jet are 20 times stronger in the model. Essentially, the jet causing the unsteady distorted flow pattern at sump inlet was much weaker in the model test as compared to site conditions.

- The effect of the model size versus the actual size
- The correlation for flow conditions at the site versus the model, and the true interaction with the pump

Modification to Pump—Scope

At the same time that the additional model tests were being performed and evaluated (late May 1999), there was a general consensus among the engineering company, the contractor, the user, and the pump manufacturer to use a global approach covering the three major factors that were contributing to the field problem (i.e., hydraulic interaction between the sump and the pump, mechanical interaction, and acoustic interaction).

It was decided to first attack the source of the recirculation problem, which was thought to be the hydraulic interaction between the sump and the pump. Next, each side of the hydraulic interaction (suction system and pump) was reviewed with the objective of studying and eventually implementing changes for each actor (system and pump), which would result in a high

probability of almost 100 percent of solving the field problem within a time period acceptable to the user company. The mechanical and acoustic interactions (discharge system response) were not directly addressed in the initial phase, but were still present in the background. The primary emphasis was given to the hydraulic changes, which would have positive side effects on both the mechanical and acoustic responses.

Based upon the results of the model test of the as-built sump, it was recognized that the unsteady flow distortion at the impeller was the dominant cause leading to the suction recirculation. It was agreed that the practical approach was to find modifications that would allow the pump to operate in an “imperfect” sump. Therefore, any major modifications to the suction piping (changing elbows, adding turning vanes, etc.) were excluded based upon cost and production delays. Sump modifications were assumed to be a reduction, but not an elimination, of the flow distortion, even with a 40 percent probability of success.

Therefore, pump changes were also considered with the scope being to minimize the pump sensitivity to inlet flow distortions and minimize suction recirculation effects. The pump components that would effectively respond to such scope were clearly the suction bell and the impeller. The main objective for a new design bell was to act as a flow straightener correcting the residual distortion still induced by the sump (40 percent probability of success). The design objective of a new impeller was to reduce the sensitivity to inlet flow distortion and to increase the tolerance to suction recirculation (15 percent probability of success because the existing impeller already had a large margin against suction recirculation).

Next, the decision was made to immediately begin designing and manufacturing a new suction bell without waiting for the results of the modifications to the sump. The impeller design would also be started; however, a new impeller would not be manufactured until the tests were completed with the sump modifications and the new suction bell. The total probability of success with the sump modifications and new inlet bell were estimated to be approximately 80 percent. If the recirculation problem still existed after the sump modifications and the new inlet bell were installed, then a new impeller would be designed incorporating field indications with sump/bell changes and installed.

Pump Change—New Suction Bell Design

The primary design objective of the new suction bell was to make sure that the impeller (possibly the one already operating at the site) would operate properly, by completely eliminating any residual flow distortion remaining at the suction bell inlet. The first step was to have a better understanding of why the existing impeller was subjected to suction recirculation at flowrates well above the BEP, while by inherent design features this should occur well below BEP, as shown by incidence analysis with uniform inlet flow. The field data and the model test of the as-built sump revealed several factors that affected the flow at the bell throat (i.e., impeller eye), all of which having impact on flow separation inside the impeller and consequently the onset of suction recirculation.

- *Local flow deficit*—The analysis of the field static pressure distortion at the impeller inlet suggested a possible flow deficit in one region of the section. This means that the local axial velocity was below the average velocity, which reduced the relative flow angle causing the local incidence angle to become higher than the value calculated with the average axial velocity (assuming uniform flow). However, the flow capacity deficit was supposedly near 6 percent, which would have a marginal increase of the incidence angle. This shift of the local incidence angle would be insufficient to explain the observed shift of the suction recirculation capacity. For example, previous tests (Silvaggio and Spring, 1984) with flow distortion and deficits up to 25 percent caused by a side suction chamber at the P-plane were reported to have negligible impact on the flow capacity giving the peak of cavitation inception below BEP, which is close to the suction recirculation onset capacity.

- *Negative tangential velocity*—The model test showed the presence of clockwise swirl (i.e., tangential velocity component), which was opposite to the counterclockwise rotation of the impeller. This swirl reduces the flow angle and increases the incidence angle significantly. The exact amount is unknown, but this change in the incidence angle may have resulted in a stalling incidence and flow separation. Also, a negative prerotation increases the impeller vane loading and can cause an earlier flow separation.

- *Nonuniform inlet velocity profile*—The field static pressure distribution at the impeller inlet has an angular distortion (Figure 53) with shear flow. Other investigations with stationary two-dimensional diffusers have shown that nonuniform inlet velocity profiles and shear flows exhibit decreased performance when compared to diffusers having uniform inlet profiles (Wolf and Johnston, 1969). In particular, the onset of stall occurs at lower area ratios (AR) ($AR = A_{outlet}/A_{inlet}$). An impeller blade channel is like a rotating diffuser with a high AR as the positive incidence increases. Then the effect of nonuniform inlet flow is to promote the onset of stall (suction recirculation) at higher capacity than with uniform inlet velocity. In other words, the equivalent critical diffusion ratio ($1/AR$) is increased, which would raise the suction recirculation onset capacity.

- *Spanwise vane loading distribution*—The angular distortion of the pressure distribution is likely associated with a radial gradient in both velocity pressure and velocity. This increases the variation of the vane loading from hub to tip and increases the critical diffusion factor promoting earlier stall and suction recirculation (Schiavello and Sen, 1980).

- *Unsteady inlet flow*—During the model tests of the as-built sump, the vortimeter at the bell throat was unsteady suggesting an unsteady fluctuating flow is present at the impeller inlet. Boundary layers with adverse pressure gradients, especially near detachment, are certainly more unstable and more sensitive to any kind of disturbance (Custeix and Houdeville, 1983). This situation applies to the boundary layer on the suction side of the impeller blade at positive incidence, which becomes more prone to separation and early suction recirculation.

All these factors were present and combined to move the suction recirculation onset to a capacity far higher than the one likely exhibited in the shop test, and higher than expected from a theoretical analysis of the impeller design assuming steady uniform flow pattern at the bell inlet and impeller eye.

Therefore, the new suction bell was designed to correct all the above undesired flow features, if they are present by a certain extent at the bell inlet as an effect of the intake-sump flow conditions. It was recognized that the original suction inlet bell shown in Figure 60 had only a slight capability in straightening the inlet axial velocity pattern by flow acceleration, but basically it was not effective in eliminating the eventual unsteady swirling flow. Consequently, the first design modification for the new suction bell was to add a high number of internal vanes (10) with sufficiently high solidity (Figure 61). There was no concern about possible head loss, which could impair the suction performance and provoke cavitation, because the NPSHA at the site was quite high with sufficient margin above the NPSHR. Also, the head loss with properly designed guide vanes is not high (low velocity in the bell) and is predictable.

The second key design modification was to create a controlled and positive swirling flow (counterclockwise direction) with slight positive prerotation (i.e., in the same direction of the impeller rotation), which theoretically would reduce the onset and magnitude of suction recirculation. Therefore, curved vanes were used with an exit blade angle of 20 degrees (from the axial direction). This resulted in an absolute flow angle of approximately 10 degrees, which reduced the incidence angle and moved the shockless capacity even closer to the rated point.

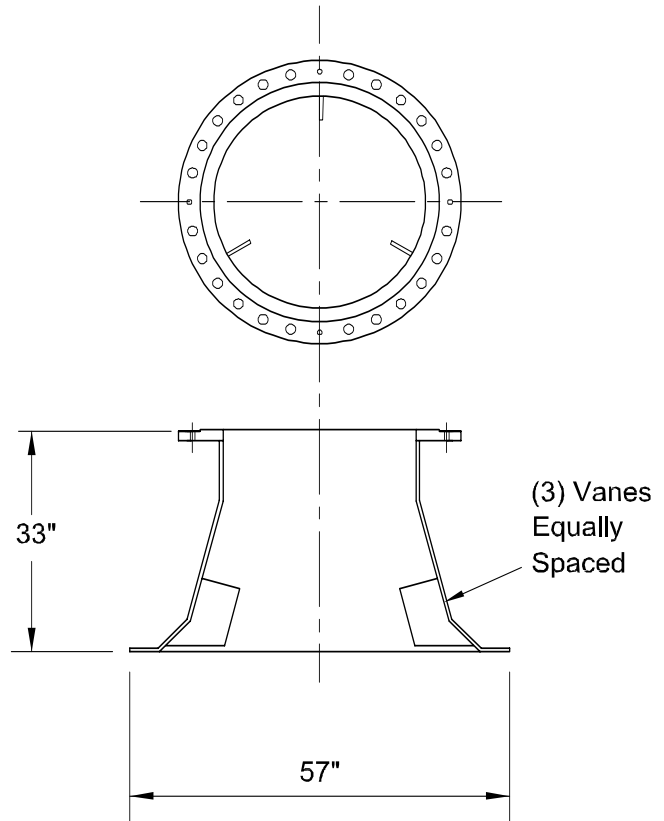


Figure 60. Sketch of Original Suction Inlet Bell.

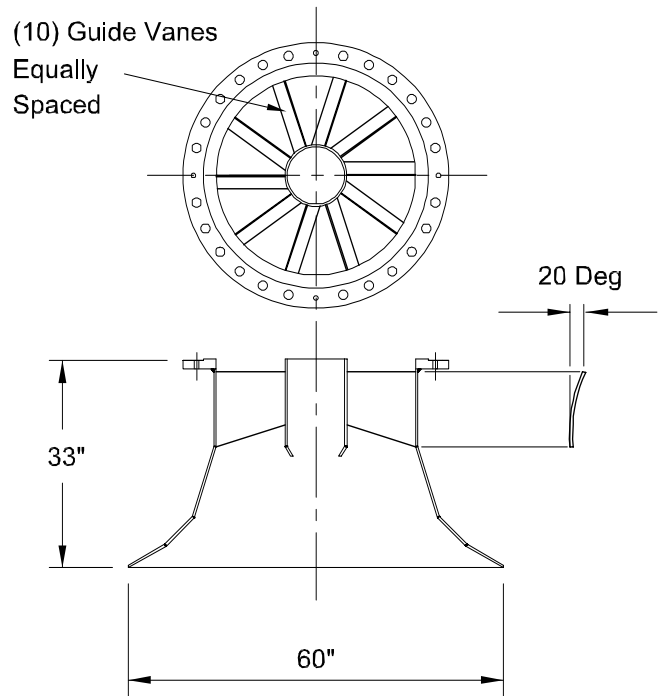


Figure 61. Sketch of Modified Suction Inlet Bell.

Further, the inlet diameter of the bell was increased for multiple reasons:

- The ratio of W_s/D_b (W_s = sump width, D_b = suction bell inlet diameter) was reduced from the original value of 2.2 to 2.0 to strictly comply with the recommended ratio value (Flowserve-IDP, 1991; ANSI/HI 9.8, 1998).

- The velocity at the suction bell inlet was reduced to make the flow inside the bell less sensitive to upstream flow turbulence and unsteadiness.
- The “net” or active area between the suction bell contour and the central wedge-shaped baffle under the pump was also increased.

The new suction bell was “custom” designed to better match the “given” sump dimensions and to filter any residual flow distortion, improper swirl, and unsteadiness resulting from the intake-sump configuration. The final design goal was to produce a flow pattern in front of the impeller that was close to the impeller design assumptions as present in the shop test arrangement, and as recommended by ANSI/HI 9.8 (1998).

Pump Change—New Impeller Design

The pump manufacturer also investigated a new impeller design that was less sensitive to inlet flow perturbations. An additional objective was to prevent the transfer of the inlet flow perturbations to the impeller outlet with risk of flow separation at the impeller inlet/bowl diffuser outlet. The main design criterion was to reduce the vane loading.

Preliminary design calculations were aimed at:

- Reducing the head coefficient by increasing the outlet diameter as untrimmed impeller
- Increasing the number of vanes from seven to eight
- Increasing the solidity by increasing the vane length and the number of vanes
- Changing the vane shape

A final impeller design was not completed because no further site modifications were required after the pump inlet bell was installed.

SOLUTION STRATEGY—FIELD IMPLEMENTATION

Field Tests with Modified Sumps

Based upon the latest model tests, the following modifications were installed in all three sumps.

- Three concrete posts (1 ft × 1 ft) were installed under the bottom of the first curtain wall extending from the sump floor to the wall bottom edge. In the model test, these posts were located in the central portion of the width to produce blockage and dissipation of the jet exiting from the flange. However, at the site, the three posts were equally spaced between the side walls.
- A sill beam was installed downstream of the trash rack. The sill beam was a concrete beam (1 ft × 1 ft) that extended across the full width of the sump and was attached to the floor.

Vibration data were measured on the pumps after these modifications were installed with the presence of one author (July 1999) using shop type instrumentation. A comparative analysis of the vibrations between May 1999 and July 1999 showed that the vibration amplitudes were lowered by 30 to 40 percent with some changes for certain frequencies (full spectra were not measured). In addition, all three pumps (A, B, and C) could be operated from high-flow down to rated-flow without showing the threatening shaking behavior observed in May 1999 without the posts.

However, the overall vibration levels remained high and were above the acceptable levels, as agreed to by all involved parties (engineering company, plant owner, maintenance operator, and the pump manufacturer). Although no pulsation data were obtained during these tests, the vibration data indicated that the suction recirculation conditions still occurred at flowrates above the BEP, although with lower intensity.

The common conclusion was that the sump modifications appeared to be much less effective than expected from the second model test. The site observations by one author, who also

witnessed the model test with the selected changes, still indicated presence of flow turbulence on each side of the main curtain wall contrary to model test observations.

Therefore, questions still remained about the correlation between the model test (scale and configuration) and the actual site flow conditions, with the focus on the effect of lack of flow simulation for the internal flows (Reynolds number similarity). In fact, the above comparison of Reynolds numbers at rated flow between prototype and model scale clearly points out that the jet flow entering into the sump was much stronger in the actual site conditions than in the model simulation (on a comparative basis at the two energy levels) with insufficient dissipation and still present near the suction bell.

Field Tests with New Suction Bell

Since the recirculation conditions were not eliminated with the sump modifications, one of the new suction bells was installed on pump A. Field tests indicated that the vibration levels were low and there was no evidence of recirculation at reduced flowrates. It would have been desirable to obtain quantitative field data of both pressure pulsation and vibration with the new inlet bell; however, since the vibration levels were low, no additional field tests were conducted.

Based upon the results with the new suction bell, identical suction bells were also installed on the other two pumps. Additional tests confirmed that the vibration levels were also reduced during two-pump operation. The vibration levels at the top of the motors were reduced to acceptable levels. In addition, the noise levels were significantly reduced, which was another confirmation that the abnormal suction recirculation problems were eliminated.

Follow-up Four Years Later

When this paper was written in summer 2003, the pumps had been in service for approximately four years since the new suction bells were installed in the fall of 1999. There was indirect knowledge that the pumps had operated satisfactorily because there had been no warranty claims from the user.

In November 2003, the plant maintenance manager was directly contacted to obtain more specific feedback and to obtain some actual vibration data on the pump. It was determined that the cooling water pumps had been in continuous service since the fall of 1999. The pumps were operated in the normal design mode with two pumps running and one in standby. Generally, pump A was operated continuously while pumps B and pump C were alternated every month. The pumps have been operating with a discharge pressure of 3.1 barg (45 psig) to 3.2 barg (46.4 psig), which was the operating condition where the suction recirculation had previously occurred before the new suction bells were installed.

Observations by plant personnel during the past four years have verified that the excessive vibration and noise levels have not reoccurred since the new suction bells were installed. These observations were confirmed with vibration data measured on the pumps and the motors. Typical vibration spectra measured on the motor bearing housing by the plant maintenance personnel are shown in Figures 62 to 64. These plots can be compared with the data obtained during the field tests with the original suction bells (Figures 20 and 43).

The frequency spectra indicated that the motor vibration levels were acceptable and occurred primarily at the mechanical natural frequencies of the pump/motor system. The vibration levels at the running speed (10 Hz) were very low and were well below the allowable levels.

According to the plant operators, the vibration levels are not constant and seem to increase when the sea conditions were rough, which was the condition on November 11, 2003, when these data were obtained. The maximum vibration levels occurred in the N-S direction at the pump column mechanical natural near 5.4 Hz, Figure 62. The motor vibrations in the E-W direction (Figure 63)

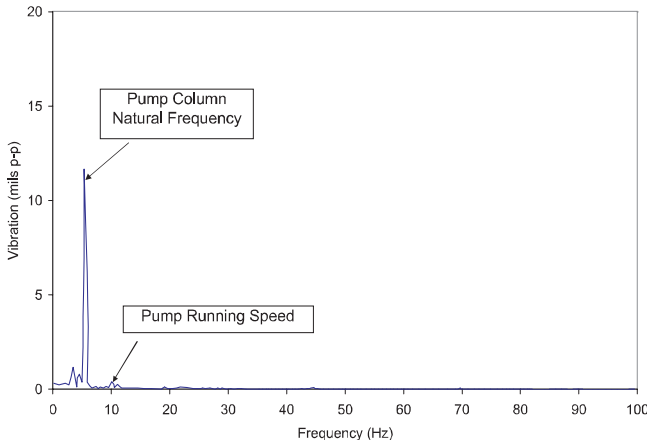


Figure 62. Frequency Spectra of Motor Vibration in N-S Direction (Follow-Up Data Obtained Four Years after Modified Suction Inlet Bell Was Installed).

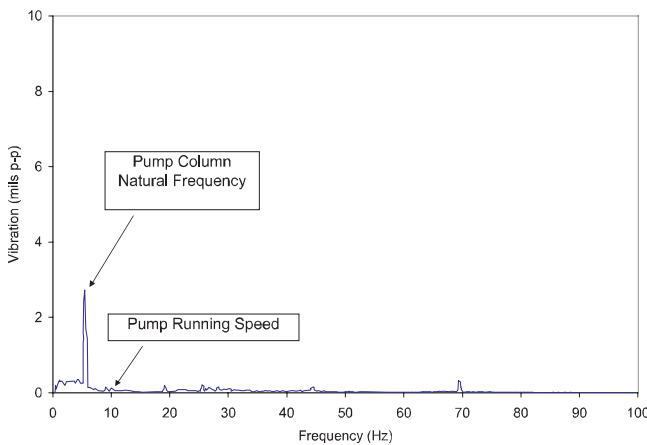


Figure 63. Frequency Spectra of Motor Vibration in E-W Direction (Follow-Up Data Obtained Four Years after Modified Suction Inlet Bell Was Installed).

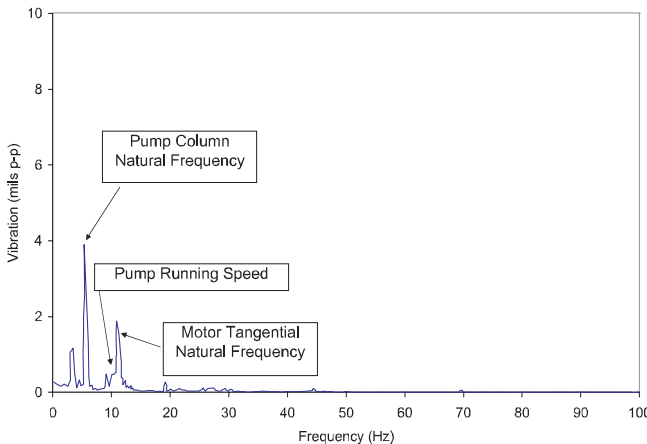


Figure 64. Frequency Spectra of Motor Vibration in Tangential Direction (Follow-Up Data Obtained Four Years after Modified Suction Inlet Bell Was Installed).

were primarily at the pump column natural frequency near 5.2 Hz and at the impeller vane passing frequency near 70 Hz. The motor vibrations in the tangential direction (Figure 64) were primarily at the pump column natural frequency near 5 Hz and at the motor twisting natural frequency near 11 Hz.

Evidently the sea agitation induces oscillations of the water level in each sump resulting in unsteady flows at the suction bell inlet, which in turn excites the mechanical natural frequencies of the pump column at 5.2 Hz and 5.4 Hz, and the motor twisting natural frequency near 11 Hz. The vibration data indicated that the guide vanes in the new suction bell did not totally eliminate the unsteadiness of the inlet flow, but were still highly effective in limiting the overall vibrations to satisfactory levels. On the other hand, the equalizing and straightening action of the guide vanes on the approaching upstream flow was fully effective as shown by the absence of suction recirculation related frequencies from the vibration spectra and also the deactivation of the acoustic/structural resonance near 11 Hz.

GENERAL CONCLUSIONS

- Pump suction recirculation was clearly observed at flowrates above the BEP in a field installation with wet pit vertical turbine pumps. To the authors' knowledge, this event was never reported in the published literature and also is apparently in contrast with pump designers' experience.
- Pumps can operate satisfactorily on the test stand and then experience problems after they are installed at the site due to improper inlet flow conditions.
- Flow visualization and quantitative measurements performed with the sump model tests indicated a sudden change of the flow pattern in the sump causing an unsteady swirling flow inside the suction bell up to the impeller eye, which may strongly affect the onset of suction recirculation.
- The change of flow regime in the open sump was occurring at a threshold capacity, which was likely due to a fluid interaction between the intake internal flows (governed by the Reynolds number) and the sump free-surface flows (governed by the Froude number). This "critical" intake/sump interaction would need confirmation with further investigations.
- The intake-sump fluid interaction has strong practical importance, because it has implications regarding the key factors for model tests (fluid similarity criterion, model scale factor, and model optimization) and also the correlation with actual site flow conditions.
- The onset and intensity of suction recirculation for centrifugal pumps with radial outlet impellers are different compared to pumps with mixed-flow impellers for the same Ns. Therefore, certain criteria used to evaluate the potential for suction recirculation in centrifugal pumps, such as suction energy and suction specific speed, are not applicable to vertical turbine pumps.
- Recirculation will occur on the test stand as the flowrates are reduced to measure the flow-head curve, but may not be noticed unless the pulsation generated by the recirculation excites a mechanical natural frequency of the pump or motor. For certain pumps, the head (power) curve may give "gross" qualitative indications. However, accurate direct detection of pressure pulsations with dynamic pressure transducers should always be made on the test stand and on site during the pump commissioning. Frequency spectra should be obtained to determine the amplitude and frequencies of the pulsation and vibration data.
- The magnitude of the pulsation and noise levels at the onset capacity are worse with high-energy pumps.
- High-energy pumps are sensitive to the inlet flow conditions. Uneven flow into the pump inlet can cause the flowrates to be significantly lower in various sections of the impeller.
- Recirculation occurs instantly within one pump rotation at a threshold flowrate, with a character of rotating stall having sub-synchronous frequencies. The resulting high-level pulsation can excite interaction with the entire pump/piping system from the sump, through the pump, and throughout the discharge piping.

- The frequencies of recirculation induced pulsation are determined by the acoustic natural frequencies of the entire pump/piping system. The acoustic natural frequencies of the pump/piping system are controlled by the geometry of the system, the speed of sound of the fluid, and the stiffness of the expansion joints.

- The pump recirculation typically generates broadband turbulence (random, low-amplitude, nonsynchronous pulsation over a large frequency range from 1 to 2000 Hz). In addition to exciting the acoustic natural frequencies, the broadband turbulence can also excite the mechanical natural frequencies of the pump and motor, and the lateral natural frequencies of the pump rotor.

- The vibration levels are further increased when the acoustic natural frequencies are coincident with the mechanical natural frequencies.

- Modifications to pump inlet bell (guide vanes, larger diameter, etc.) can correct possible flow distortion of the upstream approaching flow and improve the flow uniformity/steadiness at the impeller inlet.

- Changing the acoustical natural frequencies of the piping system, changing the pump structural natural frequencies, or in principle eliminating the recirculation are all potential solutions to reduce the vibration of the pump/motor/piping system. However, generally the preferred solution is to reduce the excitation by just shifting the recirculation outside the normal operating range and also correcting in a practical way the inlet flow disturbance induced by the suction system.

- Circumferential variation of the static pressure measurements in the suction bell is indicative of unexpected inlet flow distortion.

- Recirculation was identified by:

- Sudden increase in the suction static pressure as the discharge pressure was increased and flow reduced,

- Sudden increase in nonsynchronous pulsation in suction and discharge as the discharge pressure was increased and flow reduced,

- Sudden increase in nonsynchronous vibration of the pump, motor, and piping as the discharge pressure was increased and flow reduced,

- Sudden increase in nonsynchronous motor amps as the discharge pressure was increased and flow reduced, and

- Sudden backflow observed in underwater videos of the pump inlet.

ACKNOWLEDGEMENTS

The authors would like to acknowledge the management at Flowserve Pump Division and Engineering Dynamics Incorporated for permitting the publication of this paper. Additionally, they would like to recognize the contribution to the field measurements and data analysis provided by: T. Wotring (Flowserve Pump), F. Antunes (formerly with IDP), and W. Marscher (Mechanical Solution Inc.).

REFERENCES

- ANSI/HI 2.1-2.5, 1994, "Vertical Pumps for Nomenclature, Definitions, Application and Operation," Hydraulic Institute, Parsippany, New Jersey.
- ANSI/HI 9.6.1, 1998, "Centrifugal and Vertical Pumps for NPSH Margins," Hydraulic Institute, Parsippany, New Jersey.
- ANSI/HI 9.8, 1998, "Pump Intake Design Standards," Hydraulic Institute, Parsippany, New Jersey.
- Barrand, J. P., Caignaert, G., Canavelis, R., and Guiton, P., 1984, "Experimental Determination of the Reverse Flow Onset in a Centrifugal Impeller," *Proceedings of the First International Pump Symposium*, Turbomachinery Laboratory, Texas A&M University, College Station, Texas, pp. 63-71.
- Blevins, D. R., 1984, *Applied Fluid Dynamics Handbook*, New York, New York: Van Nostrand Reinhold Company.
- Breugelmans, F. A. E. and Sen M., 1982, "Prerotatation and Fluid Recirculation in the Suction Pipe of Centrifugal Pumps," *Proceedings of Eleventh Turbomachinery Symposium*, Turbomachinery Laboratory, Texas A&M University, College Station, Texas, pp. 165-180.
- Budris, A. R., 1993, "The Shortcomings of Using Pump Suction Specific Speed Alone to Avoid Suction Recirculation Problems," *Proceedings of the Tenth International Pump Users Symposium*, Turbomachinery Laboratory, Texas A&M University, College Station, Texas, pp. 91-95.
- Bush, A. R., Fraser, W., and Karassik, I. J., 1975, "Coping with Pump Progress: Part I—The Sources and Solutions of Centrifugal Pump Pulsations, Surges, and Vibrations," *Worthington - Pumpworld*, 1, (1).
- Bush, A. R., Fraser, W., and Karassik, I. J., 1976, "Coping with Pump Progress: Part II—Treating Internal Recirculation," *Worthington - Pumpworld*, 2, (1).
- Chauvin, J., Ferrand, P., Sen, M., and Schiavello, B., 1980, "Decollement Tournant dans les Pompes et les Compresseurs (Rotational Flow Separation in Pumps and Compressors)," (in French), *La Houille Blanche*, (1-2), pp. 69-76.
- Claxton, J., Hecker, G. E., and Sdano, A., 1999, "The New Hydraulic Institute Pump Intake Design Standard," *Proceedings of the Sixteenth International Pump Users Symposium*, Turbomachinery Laboratory, Texas A&M University, College Station, Texas, pp. 161-169.
- Colpin, J., 1977, "Inlet Flow Distortions in Axial Flow Compressors," VKI TN 122, Rhode-St-Genese, Belgium.
- Custeix, J. and Houdeville, R., 1983, "Effects of Unsteadiness on Turbulent Boundary Layers in Turbulent Shear Flows," VKI LS 1983-03, Rhode-St-Genese, Belgium.
- Daggett, L. and Keulegan, G. H., 1974, "Similitude in Free-Surface Vortex Formation," *ASCE Journal of the Hydraulics Division*, 100, (HY11), p. 1565.
- Dicmas, L. J., 1987, *Vertical Turbine, Mixed-Flow & Propeller Pumps*, New York, New York: McGraw-Hill Book Company.
- Ferrini, F., 1974, "Some Aspects of Self-Induced Prerotatation in the Suction Pipe of Centrifugal Pump in Pumps and Pumping Systems for Liquids in Single or Multiphase Flow," H. Worthington European Technical Award 1973, First Edition, 3, Hoepli, Milan, Italy, pp. 1-27.
- Flowserve-IDP, 1991, "Test Standards for Pump Model Intakes," Engineered Pump Division, Phillipsburg, New Jersey.
- Fraser, W. H., 1981, "Recirculation in Centrifugal Pumps," *Materials of Construction of Fluid Machinery and Their Effect on Design and Performance*, ASME, pp. 65-86.
- Fraser, W. H., 1983, "Suction—Discharge Recirculation," Private Conversations.
- Gatz, A., 1999, "Intake—Sump Design," Private Conversations.
- Hallam, J. L., 1982, "Centrifugal Pumps: Which Suction Specific Speeds are Acceptable," *Hydrocarbon Processing*.
- Hecker, G. E., 1981, "Model Prototype Comparison of Free Surface Vortices," *ASCE Journal of the Hydraulic Division*, 107, (HY10), p. 1243.
- Idelcik, I. E., 1969, *Memento des Pertes de Charge*, Paris, France: Eyrolles Editeur.

- Janigro, A. and Schiavello, B., 1978, "Prerotation in Centrifugal Pumps. Design Criteria in Off-Design Performance of Pumps," VKI LS 1978-3, Rhode-St-Genese, Belgium.
- Karassik, I. J., 1981, *Centrifugal Pump Clinic*, New York, New York: Marcel Dekker, Inc.
- Karassik, I. J., Messina, J. P., Cooper, P., and Heald, C. C., 2001, *Pump Handbook*, Third Edition, New York, New York: McGraw-Hill Inc.
- Kaupert, K. A. and Staubli, T., 1999a, "The Unsteady Pressure Field in a High Specific Speed Centrifugal Pump Impeller—Part I: Influence of the Volute," Transactions of ASME, Journal of Fluids Engineering, pp. 621-626.
- Kaupert, K. A. and Staubli, T., 1999b, "The Unsteady Pressure Field in a High Specific Speed Centrifugal Pump Impeller—Part II: Transient Hysteresis in the Characteristic," Transactions of ASME, Journal of Fluids Engineering, pp. 627-632.
- Knauss, J., 1987, Swirling Flow Problems at Intakes," *IAHR Hydraulic Structures Design Manual*, Rotterdam, The Netherlands: A.A. Balkema Publishers.
- Massey, I. C., 1976, "The Suction Instability Problem in Rotordynamic Pumps," *Proceedings of International Conference on Design and Operation of Pumps and Turbines*, Paper 4.1, NEL, East Kilbride, Glasgow, United Kingdom.
- Miller, D. S., 1979, *Internal Flow Systems*, BHRA Fluid Engineering, Cranford, United Kingdom.
- Minami, S., Kawaguchi, K., and Homma, T., 1960, "Experimental Study on Cavitation in Centrifugal Pump Impellers," Bulletin of JSME, 3, (9), pp. 9-19.
- Murakami, M. and Heya, N., 1966, "Swirling Flow in Suction Pipe of Centrifugal Pumps-1st Report: Distribution of Velocity and Energy," Bulletin of JSME, 9, (3), p. 328.
- Murakami, M. and Heya, N., 1969, "Improvement of Pump Performance by Impeller Eye Throttling," ASME Paper 69-FE-26.
- Padmanabhan, M. and Hecker, G. E., 1984, "Scale Effects in Pump Sump Models," ASCE Journal of Hydraulic Engineering, 110, (11), p. 1540.
- Prosser, M. J., 1977, "The Hydraulic Design of Pump Sumps and Intakes," BHRA Fluid Engineering, Cranford, United Kingdom.
- Rey, R., Guiton, P., Kermarec, and Vullioud, G., 1982, "Etude Statistique sur les Caracteristique a Debit Partiel des Pompes Centrifuges et sur la Determination Approximative du Debit Critique (Statistical Study of Partial Flow Characteristics of Centrifugal Pumps and of Approximate Determination of the Critical Flow)," *La Houille Blanche*, (2-3), pp. 107-120.
- Rosenberger, H., Helmann, D. H., and Naghash, M., 1997, "Physical Model Study of Several Jet-Breaker Baffle Concepts in Pump Intake Structures with Pipe Inflows," The 27th IAHR Congress, San Francisco, California.
- Schiavello, B., 1975, "Optimization of Pump Design Based on a Parametric Study," VKI PR 1975-14, Rhode-St-Genese, Belgium.
- Schiavello, B., 1982, "Debit Critique d' Apparition de la Recirculation a l' entrée des Roues de Pompes Centrifuges: Phenomenes Determinants, Methodes de Detection, Criteres de Prevision (Critical Flow Engendering Appearance of Recirculation at Centrifugal Pump Impeller Inlet: Determinant Phenomena, Detection Methods, Forecasting Criteria)," *La Houille Blanche*, (2-3), pp. 139-158.
- Schiavello, B., 1983, "A Diffusion Factor Correlation for the Prediction of the Reverse Flow Onset at the Centrifugal Pump Inlet," *Proceedings of the Seventh Conference on Fluid Machinery*, Akademiai Kiado, Budapest, Hungary, 2, pp. 751-760.
- Schiavello, B., 1988, "Panel Session on Specifying Minimum Flow: The Impact of Fluid Dynamic Design on Minimum Flow," *Proceedings of the Fifth International Pump Users Symposium*, Turbomachinery Laboratory, Texas A&M University, College Station, Texas, pp. 186-192.
- Schiavello, B., 1993, "Cavitation and Recirculation Troubleshooting Methodology," *Proceedings of the Tenth International Pump Users Symposium*, Turbomachinery Laboratory, Texas A&M University, College Station, Texas, pp. 133-156.
- Schiavello, B. and Sen, M., 1980, "On the Prediction of the Reverse Flow Onset at the Centrifugal Pump Inlet," *Proceedings of Performance Prediction of Centrifugal Pumps and Compressors*, ASME 22nd Fluids Engineering, New Orleans, Louisiana, pp. 261-272.
- Sen, M., 1976, "Experimental Study on the Inlet Flow Field of a Centrifugal Pump," VKI PR 1976-12, Rhode-St-Genese, Belgium.
- Sen, M., 1978, "Prerotation in Centrifugal Pumps in Off-Design Performance of Pumps," VKI LS 1978-3, Rhode-St-Genese, Belgium.
- Sen, M., Breugelmanns, F.A.E., and Schiavello, B., 1979, "Reverse Flow, Prerotation and Unsteady Flow in Centrifugal Pumps," *Proceedings of Fluid Mechanics Silver Jubilee Conference*, Paper No. 3.1, NEL, East Kilbride, Glasgow, United Kingdom.
- Silvaggio, J.A. Jr. and Spring, H., 1984, "Air Model Testing to Determine Entrance Flow Fields," *Proceedings of the First International Pump Symposium*, Turbomachinery Laboratory, Texas A&M University, College Station, Texas, pp. 57-62.
- Sloteman, D. P., Cooper, P., and Dussourd, J. L., 1984, "Control of Backflow at the Inlets of Centrifugal Pumps and Inducers," *Proceedings of the First International Pump Symposium*, Turbomachinery Laboratory, Texas A&M University, College Station, Texas, pp. 9-22.
- Sulzer Pumps, 1998, *Sulzer Centrifugal Pump Handbook*, Second Edition, Oxford, United Kingdom: Elsevier Advanced Technology.
- Toyokura, T. and Kubota, N., 1968, "Studies on Back-Flow Mechanism of Turbomachines: Part 1—Back-Flow Mechanism to the Suction Side of Axial-Flow Impeller Blades," Bulletin of JSME, 11, (43), pp. 147-156.
- Toyokura, T. and Kubota, N., 1969, "Studies on Back-Flow Mechanism of Turbomachines: Part 2—Back-Flow Mechanism to the Suction Side of Mixed-Flow Impeller Blades," Bulletin of JSME, 12, (50), pp. 215-223.
- Wolf, S. and Johnston, J. P., 1969, "Effects of Nonuniform Inlet Velocity Profiles on Flow Regimes and Performance in Two-Dimensional Diffusers," Transactions of ASME, Journal of Basic Engineering, pp. 462-474.

BIBLIOGRAPHY

- Cornman, R. E., 1986, "Analytical and Experimental Techniques for Solving Pump Structural Resonance Problems," *Proceedings of the Third International Pump Symposium*, Turbomachinery Laboratory, Texas A&M University, College Station, Texas, pp. 27-32.
- Dufour, J. W. and Nelson, W. E., 1993, *Centrifugal Pump Sourcebook*, New York, New York: McGraw-Hill, Inc.

- Engineering Dynamics Incorporated (EDI), 2002, *Vibrations in Reciprocating Machinery and Piping Systems*, Eighth Printing.
- Florjancic, S. S. and Frei, A., 1993, "Dynamic Loading on Pumps—Causes for Vibration," *Proceedings of the Tenth International Pump Users Symposium*, Turbomachinery Laboratory, Texas A&M University, College Station, Texas, pp. 171-184.
- GE Water Technologies, 2003, "Understanding Pump Cavitation," <http://www.gewater.com>.
- Lobanoff, V. S. and Ross, R. R., 1985, *Centrifugal Pumps: Design and Application*, Second Edition, Houston, Texas: Gulf Publishing Company.
- Nelson, W. E. and Dufour, J. W., 1992, "Pump Vibrations," *Proceedings of the Ninth International Pump Users Symposium*, Turbomachinery Laboratory, Texas A&M University, College Station, Texas, pp. 137-147.
- Schiavello, B. and Sen., M., 1981, "Experimental Investigation on Centrifugal Pump Design Criteria for Minimum Reverse-Flow Delivery in Improvements in Turbomachines and Related Techniques," H. Worthington European Technical Award 1979, 5, Hoepli, Milan, Italy, pp. 191-239.
- Sen, M., June 1980, "Study of Inlet Flow of Centrifugal Pumps at Partial Flow Rates," Ph.D. Thesis, University of Brussels, Belgium.
- Silvaggio, J. A. Jr. and Krafft, G., 1999, "How to Extend the Life of Your Boiler Feed Pump," *Proceedings of the Sixteenth International Pump Users Symposium*, Turbomachinery Laboratory, Texas A&M University, College Station, Texas, pp. 153-160.
- Sulzer Brothers Limited, 1993, *Feedpump Operation and Design Guidelines: Summary Report*, Pleasant Hill, California: Electric Power Research Institute.